levels in C26 cells compared with normal cells. Therefore, NO-HSA may show selective cytotoxicity for tumor cells and not affect normal cells. These findings strongly suggest that NO-HSA is a promising therapeutic anticancer agent, given the unusual redox conditions typical of malignant cells.

Antiapoptotic effects of NO have been observed in a variety of cells, including T cells, hepatocytes, endothelial cells, neurons, ovarian follicle cells, eosinophils, thymocytes, and embryonic kidney cells (Liu and Stamler, 1999). In a recent study using U937 human promonocytic cells, NO-R410C (a genetic variant of HSA) had antiapoptotic activity (Ishima et al., 2007). Whether NO ultimately inhibits or promotes apoptosis probably depends on the cell, the signal, the source, the molecule, the amount, and the presence or absence of coreactants. For example, the amount of NO bound to the carrier molecule seems to account for the discrepant results between previous investigations and the present study. The NO content of NO-R410C (in the previous study) and NO-HSA (in this study) were 1.3 and 6.6 mol NO/mol HSA, respectively, and the *S*-nitroso moiety concentrations in vitro were 26 to 130 and 165 to 660 μM, respectively. Mohr et al. (1997) reported that 10 to 100 μM GSNO inhibits the activation of caspase-3 induced by actinomycin D in U937 cells. In contrast, apoptosis (characterized by DNA fragmentation and morphological changes) was observed in U937 cells treated with GSNO at concentrations in excess of 250 μM (Messmer et al., 1996). Based on the results of the present study and those of previously published investigations, the critical NO threshold concentration between promotion and inhibition of apoptosis seems to be 100 to 200 μM.

Matsumura et al. (1987) examined the accumulation of differently sized proteins within tumor tissues of tumor-bearing mice. Macromolecules containing HSA tended to accumulate in tumor tissues, apparently due to hypervascularization and enhanced vascular permeability (even to macromolecules) of the tumors, with little export of macromolecules from the tumor tissue via blood or lymphatic vessels (Matsumura et al., 1987). Therefore, NO-HSA may be a useful agent for targeting chemotherapeutics to tumor tissue. However, the short half-life of NO has been one of the greatest obstacles to therapeutic application of NO donors. Consequently, the pharmacokinetic properties of NO-HSA in mice were measured to determine the biological fate of NO. The apparent half-life of *S*-nitroso moieties in NO-HSA was estimated to be 18.9 min (data not shown), which is similar to that of NO-R410C, but much longer than that of the low-molecular-weight NO donor GSNO (4.2 min) (Ishima et al., 2007). In the present study, the difference in NO half-life between NO-HSA and GSNO seemed to be due to reduced renal excretion of HSA compared with glutathione due to its larger molecular size, suggesting that HSA may be a useful NO carrier in vivo.

In summary, NO-HSA was synthesized by inducing *S*-nitrosothiol linkages using iminothiolane as a spacer. NO-HSA generated ROS in C26 cells, and it induced intrinsic apoptotic events, such as depolarization of mitochondrial membrane potentials, activation of caspase-3, and induction of DNA fragmentation. Moreover, NO-HSA inhibited proliferation of tumor cells in vitro in a concentration-dependent manner. In the in vivo experiments, NO-HSA also strongly inhibited tumor growth by inducing apoptosis, with no side effects. The results of the present study suggest that NO-HSA has promise as a new generation anticancer agent with few side effects.

References

Azuma H, Ishikawa M, and Sekizaki S (1986) Endothelium-dependent inhibition of platelet aggregation. *Br J Pharmacol* **88:**411–415.

Beckman JS and Crow JP (1993) Pathological implication of nitric oxide, superoxide and peroxnitrite formation. *Biochem Soc Trans* **21:**330–334.

Brune B, Sandau K, and Knethen AV (1998) Apoptotic cell death and nitric oxide: activating and antagonistic transducing pathways. *Biochemistry (Mosc)* **63:**817–825.

Chen RF (1967) Removal of fatty acids from serum albumin by charcoal Treatment. *J Biol Chem* **242:**173–181.

Ewing JF, Young DV, Janero DR, Garvey DS, and Grinnell TA (1997) Nitrosylated bovine serum albumin derivatives as pharmacologically active nitric oxide congeners. *J Pharmacol Exp Ther* **283:**947–954.

Fabbri F, Brigliadori G, Ulivi P, Tesei A, Vannini I, Rosetti M, Bravaccini S, Amadori D, Bolla M, and Zoli W (2005) Pro-apoptotic effect of a nitric oxide-donating NSAID, NCX4040, on bladder carcinoma cells. *Apoptosis* **10:**1095–1103.

Feng R, Ni HM, Wang SY, Tourkova IL, Shulin MR, Harada H, and Yin XM (2007) Cyanidin-3-rutinoside, a natural polyphenol antioxidant, selectively kills leukemic cells by induction of oxidative stress. *J Biol Chem* **282:**13468–13476.

Gao J, Liu X, and Rigas B (2005) Nitric oxide-donating aspirin induces apoptosis in human colon cancer cells through induction of oxidative stress. *Proc Natl Acad Sci U S A* **102:**17207–17212.

Garthwaite J (1991) Glutamate, nitric oxide and cell-cell signaling in the nervous system. *Trends Neurosci* **14:**60–67.

Gavrieli Y, Sherman Y, and Ben-Sasson SA (1992) Identification of programmed cell death in Situ via specific labeling of nuclear DNA fragmentation. *J Cell Biol* **119:**493–501.

Hibbs JB Jr, Taintor RR, Vavrin Z, and Rachlin EM (1988) Nitric oxide: a cytotoxic activated macrophage effector molecule. *Biochem Biophys Res Commun* **157:**87–94.

Ignarro LJ (1989) Endothelium-derived nitric oxide–pharmacology and relationship to the actions of organic nitrate esters. *Pharm Res* **6:**651–659.

Ishima Y, Sawa T, Kragh-Hansen U, Miyamoto Y, Matsushita S, Akaike T, and Otagiri M (2007) *S*-Nitrosylation of human variant albumin Liprizzi (R410C) confers potent antibacterial and cytoprotective properties. *J Pharmacol Exp Ther* **320:**969–977.

Ishiyama M, Tominaga H, Shiga M, Sasamoto K, Ohkura Y, and Ueno K (1996) A combined assay of cell viability and in vitro cytotoxicity with a highly water-soluble tetrazolium salt, neutral red and crystal violet. *Biol Pharm Bull* **19:**1518–1520.

Kashfi K, Ryann Y, Qiao LL, Williams JL, Chen J, Soldato PD, Traganos FT, and Rigas B (2002) Nitric oxide-donating nonsteroidal anti-inflammatory drugs inhibit the growth of various cultured human cancer cells: evidence of a tissue type-independent effect. *J Pharmacol Exp Ther* **303:**1273–1282.

Kaufmann SH and Gores GJ (2000) Apoptosis in cancer: cause and cure. *Bioessays* **22:**1007–1017.

Kiziltepe T, Hideshima T, Ishitsuka K, Ocio EM, Raje N, Catley L, Li CQ, Trudel LJ, Yasi H, Vallet S, et al. (2007) JS-K, a GST-activated nitric oxide generator, induces DNA double-strand breaks, activates DNA damage response pathways, and induces apoptosis in vitro and in vivo in human multiple myeloma cells. *Blood* **110:**709–718.

Kondo Y, Kanzawa T, Sawaya R, and Kondo S (2005) The role of autophagy in cancer development and response to therapy. *Nat Rev Cancer* **5:**726–734.

Laval F and Wink DA (1994) Inhibition by nitric oxide of the repair protein, O6-methyl-gluanine-DNA-methyltransferase. *Carcinogenesis* **15:**443–447.

Liu L and Stamler JS (1999) NO: an inhibitor of cell death. *Cell Death Differ* **6:**937–942.

Marks DS, Vita JA, Folts JD, Keaney JF Jr, Welch GN, and Loscalzo J (1995) Inhibition of neointimal proliferation intimal proliferation in rabbits after vascular injury by a single treatment with a protein adduct of nitric oxide. *J Clin Investig* **96:**2630–2638.

Marletta MA, Yoon PS, Iyengar R, Leaf CD, and Wishnok JS (1988) Macrophage oxidation of L-arginine to nitrite and nitrate-nitric oxide is an intermediate. *Biochemistry* **27:**8706–8711.

Matsumura Y, Oda T, and Maeda H (1987) General mechanism of intratumor accumulation of macromolecules: advantage of macromolecular therapeutics. *Gan To Kagaku Ryoho* **14:**821–829.

Matsushita S, Ishima Y, Chuang VT, Watanabe H, Tanase S, Maruyama T, and Otagiri M (2004) Functional analysis of recombinant human serum albumin domains for pharmaceutical applications. *Pharm Res* **10:**1924–1932.

Messmer UK, Reimer DM, and Brune B (1996) Nitric oxide-induced apoptosis: p53-dependent and p53-indeoendent signaling pathways. *Biochem J* **319:**299–305.

Meng XW, Lee SH, and Kaufmann SH (2006) Apoptosis in the treatment of cancer: a promise kept? *Curr Opin Cell Biol* **18:**668–676.

Mohr S, Zech B, Lapetina EG, and Brune B (1997) Inhibition of caspase-3 by S-nitrosation and oxidation caused by Nitric oxide. *Biochem Biophys Res Commun* **238:**387–391.

Moncada S and Higgs A (1993) The L-arginine-nitric oxide pathway. *N Engl J Med* **329:**2002–2012.

Moncada S, Palmar RMJ, and Gryglewski RJ (1986) Mechanism of action of some inhibitors of endothelium-derived relaxing factor. *Proc Natl Acad Sci U S A* **83:**9164–9168.

Okada H and Mak TW (2004) Pathways of apoptotic and non-apoptotic death in tumor cells. *Nat Rev Cancer* **4:**592–603.

Peters T Jr (1985) Serum albumin. *Adv Protein Chem* **37:**161–245.

Ramachandran N, Root P, Jiang XM, Hogg OJ, and Mutus B (2001) Mechanism of

transfer of NO from extracellular S nitrosothiols into the cytosol by cell-surface protein disulfide isomerase. *Proc Natl Acad Sci U S A* **98:**9539–9544.

Schumacker PT (2006) Reactive oxygen species in cancer cells: live by sword, die by the sword. *Cancer Cell* **10:**175–176.

Semsroth S, Fellner B, Trescher K, Bernecker OY, Kalinowski L, Gasser H, Hallstrom S, Malinski T, and Podesser BK (2005) S-Nitroso human serum albumin attenuates ischemia/reperfusion injury after cardioplegic arrest in isolated rabbit hearts. *J Heart Lung Transplant* **24:**2226–2234.

Shimizu K, Asai T, Fuse C, Sadzuka Y, Sonobe T, Ogino K, Taki T, Tanaka T, and Oku N (2005) Applicability of anti-neovascular therapy to drug-resistant tumor: suppression of drug-resistant P388 tumor growth with neovessel-targeted liposomal adriamycin. *Int J Pharm* **296:**133–141.

Simon DI, Mullins ME, Jia L, Gaston B, Singel DJ, and Stamler JS (1996) Polynitrosylated proteins: characterization, bioactivity, and functional consequences. *Proc Natl Acad Sci U S A* **93:**4736–4741.

Stamler JS, Jaraki O, Osborne J, Simon DI, Keaney J, Vita J, Singel D, Valeri CR, and Loscalzo J (1992) Nitric oxide circulates in mammalian plasma primarily as an S-nitroso adduct of serum albumin. *Proc Natl Acad Sci U S A* **89:**7674–7677.

Trachootham D, Zhou Y, Zhang H, Demizu Y, Chen Z, Pelicano H, Chiao PJ, Achanta G, Arlinghaus RB, Liu J, et al. (2006) Selective killing of oncogenically transformed cells through a ROS-mediated mechanism by β-phenylethyl isothiocyanate. *Cancer Cell* **10:**241–252.

Williams JL, Borgo S, Hasan I, CastilloE, Traganos F, and Rigas B (2001) Nitric oxide-releasing nonsteroidal anti-inflammatory drugs (NSAIDs) alter the kinetics of human colon cancer cell lines more effectively than traditional NSAIDs: implication for colon cancer chemoprevention. *Cancer Res* **61:**3285–3289.

Wong PS and Fukuto JM (1999) Reaction of organic nitrate esters and S-nitrosothiols with reduced flavins: a possible mechanism of bioactivation. *Drug Metab Dispos* **27:**502–509.

Address correspondence to: Dr. Masaki Otagiri, Department of Biopharmaceutics, Graduate school of Pharmaceutical Sciences, Kumamoto University, 5-1 Oe-honmachi, Kumamoto 862-0973, Japan. E-mail: otagirim@gpo.kumamoto-u.ac.jp

Available online at www.sciencedirect.com
ScienceDirect
Biochimica et Biophysica Acta 1772 (2007) 1192–1198
www.elsevier.com/locate/bbadis

The ligand activity of AGE-proteins to scavenger receptors is dependent on their rate of modification by AGEs

Ryoji Nagai [a,*], Katsumi Mera [a,b], Keisuke Nakajou [a,b], Yukio Fujiwara [a], Yasunori Iwao [b], Hiroki Imai [c], Toshinori Murata [c], Masaki Otagiri [b]

[a] Department of Medical Biochemistry, Faculty of Medical and Pharmaceutical Sciences, Kumamoto University, Honjo, 1-1-1, Kumamoto 860-8556, Japan
[b] Department of Biopharmaceutics, Graduate School of Pharmaceutical Sciences, Kumamoto University, Japan
[c] Department of Ophthalmology, Shinshu University School of Medicine, Japan

Received 21 July 2007; received in revised form 28 August 2007; accepted 12 September 2007
Available online 17 October 2007

Abstract

The cellular interaction of proteins modified with advanced glycation end-products (AGEs) is believed to induce several different biological responses, which are involved in the development of diabetic vascular complications. We report here that the ratio of protein glycation is implicated in its ligand activity to scavenger receptors. Although highly-modified AGE-bovine serum albumin (high-AGE-BSA) was significantly recognized by human monocyte-derived macrophages and Chinese hamster ovary cells which overexpress such scavenger receptors as CD36, SR-BI (scavenger receptor class B type-I), and LOX-1 (Lectin-like Ox-LDL receptor-1), the mildly-modified-AGE-BSA (mild-AGE-BSA) did not show any ligand activity to these cells. Furthermore, when ^{111}In-labeled high- or mild-AGE-BSA were injected into the tail vein of mice, the high-AGE-BSA was rapidly cleared from the circulation whereas the clearance rate of the mild-AGE-BSA was very slow, similar to the native BSA. These results demonstrate the first evidence that the ligand activity of the AGE-proteins to the scavenger receptors and its pharmacokinetic properties depend on their rate of modification by AGEs, and we should carefully prepare the AGE-proteins *in vitro* to clarify the physiological significance of the interaction between the AGE-receptors and AGE-proteins.

Keywords: Advanced glycation end products (AGEs); N^{ε}-(carboxymethyl)lysine (CML); Scavenger receptor; Macrophage; Atherosclerosis; Diabetes

1. Introduction

The interaction between proteins modified with advanced glycation end-products (AGEs) and the scavenger receptor(s) of macrophages and smooth muscle cells is known to induce the production of several cytokines such as plasminogen activator and transforming growth factor-beta [1]. Furthermore, glycolaldehyde-derived AGE-low-density lipoprotein (AGE-LDL) induces foam cell formation from macrophages [2]. These findings suggest the role of the AGE-modified proteins and lipoproteins in the pathogenesis of atherosclerosis. However, AGE-proteins are prepared in each research group independently with different protocols, and all researchers, including our group, use excessively high concentrations of glucose and aldehydes. For instance, we prepared highly-modified AGE-bovine serum albumin (high-AGE-BSA) by incubating BSA with 1600 mM glucose for 40 weeks, or 33 mM glycolaldehyde for 7 days [3], and demonstrated that high-AGE-BSA is recognized by SR-A (class A scavenger receptor types I and II) [4], CD36 [5], SR-BI (scavenger receptor class B type-I) [6], and LOX-1 (Lectin-like Ox-LDL receptor-1) [7]. Schmidt et al. demonstrated that AGE-BSA, prepared by incubating BSA with 250 mM glucose-6-phosphate for 4 weeks, is recognized by RAGE (receptor for AGE) [8] and the cellular interactions of AGEs with RAGE are known to induce several cellular phenomena including the expression of vascular cell adhesion molecule-1 (VCAM-1) in

Abbreviations: AGE(s), advanced glycation end products; BSA, Bovine serum albumin; High-AGE-BSA, highly modified AGE-BSA; Mild-AGE-BSA, Mildly modified AGE-BSA; GA-AGE-BSA, Glycolaldehyde-derived AGE-BSA; MALDI-TOFMS, Matrix Assisted Laser Desorption/Ionization-Time of Flight Mass Spectrometry; CML, N^{ε}-(carboxymethyl)lysine; ELISA, enzyme-linked immunosorbent assay; PBS, phosphate-buffered saline

* Corresponding author. Tel.: +81 96 373 5071; fax: +81 96 364 6940.
E-mail address: nagai-883@umin.ac.jp (R. Nagai).

0925-4439/$ - see front matter © 2007 Elsevier B.V. All rights reserved.
doi:10.1016/j.bbadis.2007.09.001

endothelial cells [9], and cytokines in monocytes [10]. Vlassara and her colleagues prepared AGE-BSA by incubating BSA with 50 mM glucose-6-phosphate for 6 weeks [11] and demonstrated that AGE-receptor 1 (AGER1), a 50-kDa type A integral membrane protein with a short internal domain, suppresses cell oxidant stress and activation signaling via the EGF receptor [12]. Furthermore, Takeuchi et al. also demonstrated that AGE-BSA prepared using an unphysiologically high concentration of glyceraldehydes results in toxicity to the vascular wall cells and cortical neurons [13]. Taken together, those reports demonstrate that the AGE-proteins were prepared with unphysiologically high concentrations of aldehydes and then were employed for the cellular experiments. However, little is known about the correlation of the ligand activity of AGE-proteins and its rate of modification. In the present study we prepared mildly modified AGE-BSA (mild-AGE-BSA) by incubating BSA with 50 mM glucose for 24 weeks, and then compared its ligand activity with high-AGE-BSA against the scavenger receptors.

2. Materials and methods

2.1. Chemicals

D-glucose was purchased from Sigma-Aldrich Japan (Tokyo). Fatty acid-free bovine serum albumin (BSA) was purchased from Wako (Osaka, Japan). Lipopolysaccharide (LPS) from *Escherichia coli* was purchased from Sigma-Aldrich Japan (Tokyo). Na ^{125}I was obtained from Amersham Biosciences (Arlington Heights, IL). Tissue culture medium was from Gibco BRL (NY, USA). All other chemicals were of the best grade available from commercial sources.

2.2. Preparation of AGE-modified BSA

High-AGE-BSA was prepared as described previously [1,3]. Briefly, 0.2 g/ml of fatty acid-free BSA was dissolved in 0.5 M sodium phosphate buffer (pH 7.4) with 1.6 M of D-glucose, sterilized by ultrafiltration and incubated at 37 °C for 40 weeks, followed by dialysis against PBS. Mild-AGE-BSA was prepared by incubating 0.05 g/ml of fatty acid-free BSA with 50 mM of glucose in a 0.05 M sodium phosphate buffer (pH 7.4) at 37 °C for 24 weeks, followed by dialysis against PBS. The glycolaldehyde-derived AGE-BSA (GA-AGE-BSA) was prepared by incubating 2 mg/ml of fatty acid-free BSA with 30 mM of GA in a 0.05 M sodium phosphate buffer (pH 7.4) at 37 °C for up to 7 days, and aliquots of the samples were collected at 3 h, 6 h, 12 h, 24 h, 48 h, 96 h, and 168 h, followed by dialysis against PBS. The extent of lysine modification of the proteins was determined by reaction with 2, 4, 6-trinitrobenzenesulphonic acid as described previously [3].

2.3. Characterization of aldehyde-modified proteins

The lysine and N^{ε}-(carboxymethyl)lysine (CML) contents in the AGE-BSA and human lens samples were quantified by high performance liquid chromatography (HPLC) after acid hydrolysis with 6 N HCl for 24 h at 110 °C, as described previously [14]. The molecular mass of the AGE-BSA was measured as described previously [15]. Briefly, 1 μl of the sample protein solution (10 pmol/μl) in 0.1% aqueous trifluoroacetic acid (TFA) water was applied on a sample spot in a steel plate slide and dried in a stream of warm air. The matrix solution which contained 10 mg/ml 3,5-dimethoxy-4-hydroxycinnanic acid (sinapinic acid) (Sigma-Aldrich Japan) in 50% vol/vol ethanol in 0.1% vol/vol TFA was applied on a dried sample spot then dried in a stream of warm air again. The molecular mass of the sample was analyzed by Matrix Assisted Laser Desorption/Ionization-Time of Flight Mass Spectrometry (MALDI-TOFMS) (Shimadzu/Kratos Kompact MALDI III mass spectrometer, Kyoto, Japan), operating in the positive high energy linear mode. An agarose gel electrophoresis was performed using the Universal Gel/8 electrophoresis kit (Ciba-Corning, Tokyo), followed by staining with Coomassie brilliant blue. Their electrophoretic mobilities relative to native BSA were expressed as the relative electrophoretic mobility.

2.4. Enzyme-linked immunosorbent assay (ELISA)

ELISA was performed as described previously [16]. Briefly, each well of a 96-well microtiter plate was coated with 100 μl of the sample to be tested in PBS, blocked with 0.5% gelatin, and washed three times with PBS containing 0.05% Tween 20 (washing buffer). The wells were incubated with 0.1 ml of monoclonal anti-AGE antibody (6D12: 0.5 μg/ml) dissolved in washing buffer for 1 h. The wells were then washed with washing buffer three times and reacted with HRP-conjugated anti-mouse IgG antibody, followed by reaction with 1,2-phenylenediamine dihydrochloride. The reaction was terminated by the addition of 0.1 ml of 1 M sulfuric acid, and the absorbance at 492 nm was read by a micro-ELISA plate reader. We recently reported that 6D12 significantly recognizes CML and N^{ε}-(carboxyethyl)lysine [16].

2.5. Cellular assays

The modified BSA preparations were radiolabeled with ^{125}I using Iodo-Gen (Pierce, Rockford, IL) and dialyzed against PBS. The CHO cells overexpressing CD36, SR-B1, or LOX-1 were maintained in Ham's F-12 medium containing 10% fetal calf serum and 0.5 mg/ml of G418 (medium A). For the uptake experiments, these cells were seeded in a 24-well plate (8×10^4/well) and cultured for 2 days in 1.0 ml of medium A, which was then replaced by medium B (Dulbecco's modified Eagle's medium containing 3% BSA). Human peripheral mononuclear cells were isolated from the blood of healthy volunteers by Ficoll density gradient centrifugation (Ficoll-Paque, Amersham Biosciences). The purified monocytes were suspended in RPMI 1640 and seeded in a 24-well plate (5×10^5 cells/well) and incubated for 1 h. The monolayers thus formed were washed three times with 1.0 ml of PBS. The cells were incubated for 7 days to differentiate into macrophages and then replaced by medium B for the uptake experiments [17]. The cells in each well were incubated at 37 °C for 8 h in 0.5 ml of medium B with three different concentrations of ^{125}I-high-AGE-BSA or ^{125}I-mild-AGE-BSA, in the presence or absence of their 50-fold unlabeled ligands. To measure the cell-associated radioactivity, each well was washed twice with 1.0 ml of ice-cold PBS containing 1% BSA and two more times with ice-cold PBS. The cells were lysed with 1.0 ml of 0.1 N sodium hydroxide for 1 h at 37 °C to determine the cell-bound radioactivity and cellular proteins. The protein concentration was measured by bicinchoninic acid protein assay reagent (Pierce). The radioactivity of the sample was determined by gamma counter (ARC 360, Aloka, Tokyo, Japan). The specific association and degradation were determined by subtracting the nonspecific value from the total value [3].

2.6. Human lens samples

The human cataract lens samples were obtained after receiving the approval of the institutional review board of Shinshu University and Kumamoto University and obtaining informed consent from all patients. The fragments of lenses with cataract (8 from diabetes and 9 from non-diabetes) were collected while surgery, and then the protein concentration of the sample was measured with bicinchoninic acid protein assay reagent (Pierce, Rockford, IL). The CML content of each sample was measured by an amino acid analysis as described above.

2.7. Clearance experiments

The experimental protocol was approved by the local ethics review committee for animal experimentation. The BSA, mild-AGE-BSA, and high-AGE-BSA were radiolabeled with ^{111}In using the bifunctional chelating reagent Diethylenetriamine-*N,N,N',N'',N''*-pentaacetic acid (DTPA) anhydride, according to the method of Hnatowich et al. [18]. The mice received tail vein injections of ^{111}In-labeled proteins in saline, at a dose of 1 mg/kg. At the appropriate intervals after the injection, blood was collected from the vena cava under anesthesia, and plasma was obtained by centrifugation. The organs were

excised, rinsed with saline and weighed. The radioactivity of each sample was measured in a well-type NaI scintillation counter (ARC-500, Aloka, Tokyo). In this study, the radioactivity of all samples and that of the plasma was normalized to the percentage of dose. The plasma concentrations were analyzed by a biexponential function using the non-linear least-squares computer program MULTI [19]. The two-compartment model was fitted according to the Akaike information criterion. The tissue distribution patterns were evaluated using tissue uptake clearances (CL_{uptake}) according to the integration plot analysis. CL_{uptake} was calculated by:

$$CL_{uptake} = \frac{X_t/C_t}{AUC_{0-t}/C_t}$$

where X_t is the tissue accumulation at time t, AUC_{0-t} is the area under the plasma concentration time-curve from time 0 to t, and C_t is the plasma concentration at time t. CL_{uptake} was obtained from the slope of the plot of X_t/C_t versus AUC_{0-t}/C_t. Each data point represents the mean±SD for three mice.

2.8. Statistical analysis

All of the experimental data are expressed as the mean±SD. The differences between groups were examined for statistical significance using either Student's *t*-test or one-way analysis of variance (ANOVA) with the Newman–Keuls *post-hoc* test. A P value less than 0.05 was considered to denote the presence of a statistically significant difference.

3. Results and discussions

3.1. Physicochemical properties of AGE-BSA

We first measured the increase in the molecular weight of AGE-BSA by a MALDI TOF mass analysis. As shown in **Fig. 1**A–C, the molecular mass of mild- and high-AGE-BSA were 658 Da and 9389 Da, respectively, and were larger than the native BSA. The net negative charge of AGE-BSA was determined by an agarose gel electrophoresis. The electrophoretic mobility of the high-AGE-BSA toward the anode was significantly higher than that of the unmodified BSA, whereas the mild-AGE-BSA slightly increased its mobility (**Fig. 1**D). Therefore, it is likely that the increase in the molecular weight and the negative charge of the high-AGE-BSA was strikingly higher than that of the mild-AGE-BSA. We next measured the reactivity of 6D12 to AGE-BSA. As shown in **Fig. 1**E, 6D12 significantly recognized both the high- and mild-AGE-BSA.

In the next step, the AGE-BSA and the human lens samples were subjected to HPLC to compare the content of CML, a major AGE structure, between the physiological samples and the AGE-BSA, which was prepared *in vitro*. For this purpose,

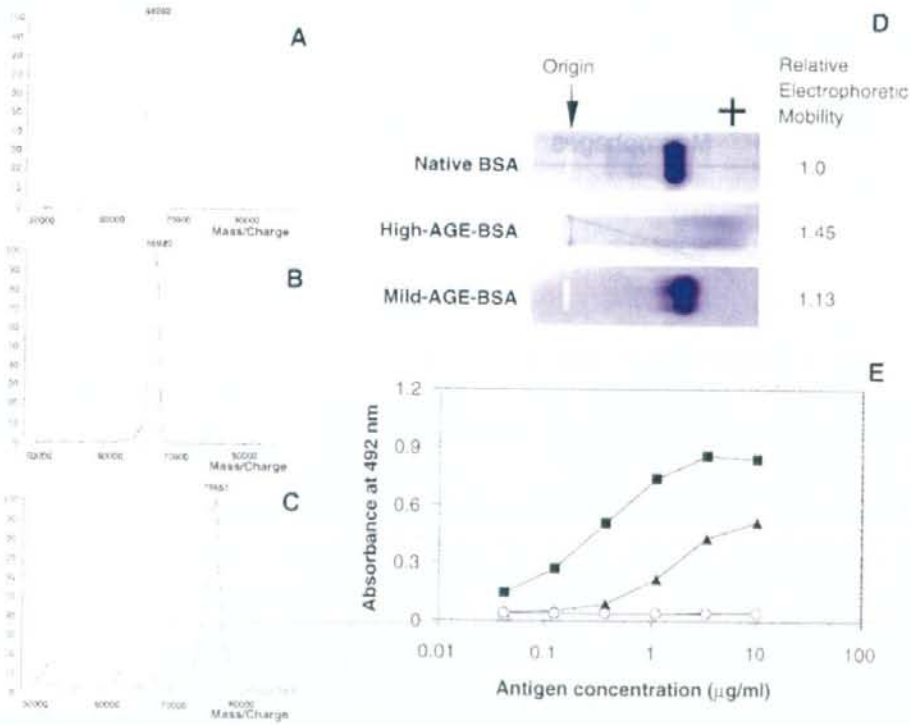

Fig. 1. Physicochemical properties of AGE-BSA. A MALDI-TOFMS analysis of native BSA (A), mild-AGE-BSA (B), and high-AGE-BSA (C). The molecular mass of the sample was analyzed by MALDI III mass spectrometer. (D) Agarose gel electrophoresis of AGE-BSA. Native BSA, mild-AGE-BSA, and high-AGE-BSA were subjected to agarose gel electrophoresis and stained with Coomassie brilliant blue. Their electrophoretic mobilities relative to native BSA were expressed as relative electrophoretic mobility. (E) The reactivity of mild- and high-AGE-BSA with 6D12 was determined by ELISA.

Table 1
Comparison of the CML content in the samples by HPLC

Samples	mmol CML/mol Lys
High-AGE-BSA	618.6
Mild-AGE-BSA	24.4
Diabetic lenses, $n=8$	17.4±3.8
Non-diabetic lenses, $n=9$	8.6±2.1

The samples were hydrolyzed with 6 N HCl for 24 h at 110 °C and then were subjected to HPLC. The amount of CML content was normalized to the lysine content of the sample. Data are mean±SD.

the human lens proteins were chosen because high amounts of AGE accumulation are observed in the long-lived proteins such as the lens proteins [20]. Table 1 summarizes the CML content in the samples. The CML content for the high- and mild-AGE-BSA were 618.6 mmol CML/mol Lys and 24.4 mmol CML/mol Lys, respectively. However, the CML contents for the diabetic- and non-diabetic human lens samples were ~17.4 mmol /mol Lys and ~8.6 mmol/mol Lys, respectively, thus indicating that our experimentally prepared mild-AGE-BSA was already more profoundly modified than physiological samples.

3.2. Ligand activity of AGE-BSA to human monocyte-derived macrophages and CHO cells overexpressing scavenger receptors

We next determined whether the high- and mild-AGE-BSA preparations could interact with cells as ligands. As shown in Fig. 2A, the ^{125}I-high-AGE-BSA was specifically associated in a dose-dependent manner, whereas these changes were not observed in the ^{125}I-mild-AGE-BSA. Similar tendencies were observed in the CHO overexpressing scavenger receptors. Therefore, the ^{125}I-high-AGE-BSA was specifically associated with the CHO cells overexpressing SR-BI (Fig. 2B), CD36 (Fig. 2C), and LOX-1 (Fig. 2D), whereas the association of the ^{125}I-mild-AGE-BSA to these cells was negligible, and thereby strongly demonstrated that only the high-AGE-BSA showed ligand activity to the scavenger receptors.

3.3. Plasma clearance and organ distribution of AGE-BSA

Fig. 3 shows the plasma clearance and organ distribution in the mice that had been intravenously injected with ^{111}In-BSA, ^{111}In-mild-AGE-BSA, and ^{111}In-high-AGE-BSA. The plasma clearance rates of ^{111}In-mild-AGE-BSA were very slow, similar to the ^{111}In-BSA, whereas the radioactivity of ^{111}In-high-AGE-BSA was rapidly cleared from the circulation, with about 90% of the injected ^{111}In-high-AGE-BSA being eliminated within 5 min after the intravenous administration (Fig. 3A). At 120 min after the intravenous injection of ^{111}In-high-AGE-BSA, the organ distribution was 60% for the liver, 1.5% for the spleen, and 4% for the kidney, suggesting that the rapid disappearance of the ^{111}In-high-AGE-BSA from the plasma is accompanied by a very pronounced increase in liver clearance (Fig. 3B–D). The uptake clearance calculated using the nonlinear least-squares

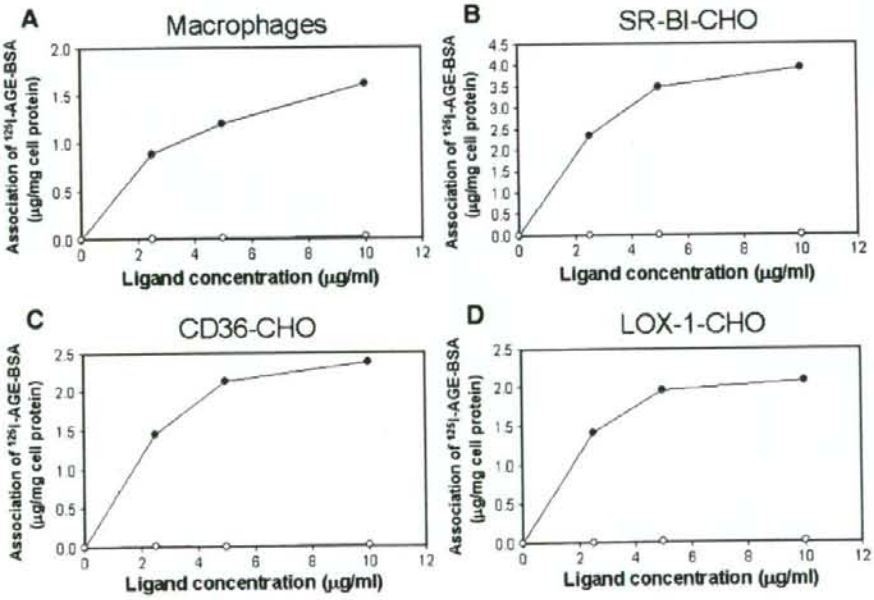

Fig. 2. Ligand activity of AGE-BSA to human monocyte-derived macrophages and CHO cells overexpressing scavenger receptors. The endocytic uptake of AGE-BSA by human monocyte-derived macrophages and CHO cells which overexpress CD36, SR-BI, and LOX-1. Human monocyte-derived macrophages (A), SR-B1-CHO (B), CD36-CHO (C), and LOX-1-CHO (D) cells were incubated at 37 °C for 8 h with the indicated concentration of ^{125}I-high-AGE-BSA (closed circles) or ^{125}I-mild-AGE-BSA (open circles) in the presence or absence of their 50-fold unlabeled ligands. The cells specific association of ^{125}I-high-AGE-BSA and ^{125}I-mild-AGE-BSA were calculated by correcting for nonspecific cell associations. Data are mean±SD, $n=2$.

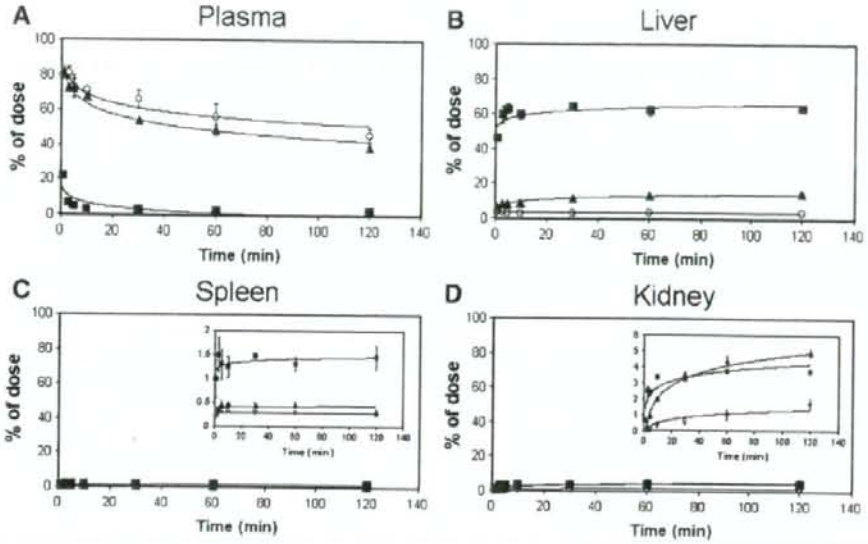

Fig. 3. Plasma clearance and organ distribution of AGE-BSA after intravenous administration to mice. ^{111}In-BSA (open circles), ^{111}In-mild-AGE-BSA (closed triangles), and ^{111}In-high-AGE-BSA (closed squares) were injected as a bolus through the tail vein of mice, and the relative radioactivities were plotted against the time after injection. Each data point represents the mean±SD for three mice.

computer program MULTI also indicated that the liver plays a major role in the clearance of high-AGE-BSA (Table 2). The accumulation by other organs such as the pancreas, lung, heart, and brain was negligibly low, and the pattern was indistinguishable from that of BSA. Since the scavenger receptors such as SR-A and SR-BI are highly expressed in the liver [21], it is reasonable to conclude that the high-AGE-BSA is endocytosed in the liver. In contrast, the clearance rate of the ^{111}In-mild-AGE-BSA was very slow in comparison to the ^{111}In-native BSA (Fig. 3A). Smedsrod et al. [22] demonstrated that intravenously injected 125I-high-AGE-BSA to rat rapidly accumulated in liver and about 60% of 125I-high-AGE-BSA was localized in endothelial cells. We also previously demonstrated that isolated mice liver endothelial cells recognize high-AGE-BSA as a ligand [23]. Those reports are correlated with our present results. Therefore, high-AGE-BSA was significantly recognized in the liver.

3.4. Correlation of the extents of lysine modification of glycolaldehyde-derived AGE-BSA with their ligand activities

Since we previously demonstrated that high-AGE-BSA and GA-AGE-BSA show the same ligand activity to the scavenger receptor [3], we next examined the correlation between the extent of the lysine modification of GA-AGE-BSA and its ligand activity to the scavenger receptor. For this purpose, we prepared the GA-AGE-BSA samples with different lysine modifications and the ^{125}I-high-AGE-BSA was incubated with RAW 264.7 cells in the presence of 50-fold unlabeled GA-AGE-BSA with different lysine modification samples. As shown in Fig. 4, although the association of ^{125}I-high-AGE-BSA to the cells was not inhibited in the presence of the 29% lysine-modified unlabeled GA-AGE-BSA, it was significantly inhibited in the presence of >49% lysine-modified unlabeled GA-AGE-BSA, demonstrating that high lysine-modification is required to be a ligand for the scavenger receptor. Furthermore,

Table 2
Uptake clearance of AGE-BSA after intravenous administration to mice

(μL/h)	Liver	Kidney	Spleen
BSA	57.5±13.1	44.4±1.9	12.6±4.8
Mild-AGE-BSA	273.3±53.8	199.1±33.0	21.9±11.6
High-AGE-BSA	35016.9±8554.4*,#	3185.3±689.6*,#	3983.8±964.4*,#

Data represent the mean±SD for three sets of experiments. *$P<0.001$ versus BSA. #$P<0.001$ versus Mild-AGE-BSA.

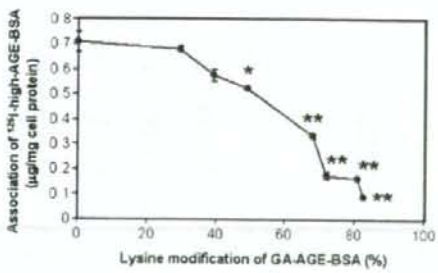

Fig. 4. Correlation of the extents of lysine modification of GA-AGE-BSA with their ligand activities. RAW 264.7 cells were incubated at 37 °C for 8 h with 1.25 μg/ml of ^{125}I-high-AGE-BSA in the presence of 50-fold unlabeled GA-AGE-BSA with different lysine modification samples. The cell association of ^{125}I-high-AGE-BSA was plotted against the extent of lysine modification of competitor GA-AGE-BSA. Data are mean±SD, $n=2$. *, $P<0.05$; **, $P<0.01$ vs. unmodified BSA.

as shown in Fig. 5, ^{125}I-GA-AGE-BSA was incubated with RAW 264.7 cells for 6 h in the presence of 50-fold excess amount of human lens samples. Although association of ^{125}I-GA-AGE-BSA was inhibited by unlabeled GA-AGE-BSA, mild-AGE-BSA and human lens samples did not show any inhibitory effect, thus indicating that physiological AGE-samples do not show any ligand activity to the scavenger receptors. Although we previously removed LPS from AGE-BSA by polylysine-conjugated sepharose column chromatography, we stopped removing LPS because the ligand activity of AGE-BSA to scavenger receptor does not change at all before and after removal of LPS. In fact, although association of ^{125}I-GA-AGE-BSA to RAW 264.7 cells was inhibited by unlabeled GA-AGE-BSA, the addition of 1–100 pg/ml of LPS did not show any inhibitory effect (Fig. 5). In the present study, we paid attention to using the fatty acid-free BSA instead of low-endotoxin BSA because Fu MX et al. [24] reported that CML is also generated from fatty acids such as arachidonate and linoleate, and thus may affect the ligand activity to scavenger receptors.

Immunohistochemical studies have demonstrated that GA-pyridine, one of the myeloperoxidase-derived AGEs through glycolaldehyde, was predominantly accumulated in the cytoplasm of the foam cells in human atherosclerotic lesions [25], thus indicating that GA-pyridine detected in foam cells may be generated within the cells. Regarding the AGE formation inside cells, Hammes et al. [26] reported that thiamine and benfotiamine prevent the intracellular AGE formation by reducing the concentration of methylglyoxal, a strong AGE-precursor, and hence inhibit diabetic retinopathy. In the case of the glycated-proteins presence *in vivo*, Thornalley et al. [15] demonstrated that end-stage renal disease is associated with a significant increase in the molecular mass of HSA (+255 Da, relative to the control subjects) and ~3% of lysine residues were modified. However, our study using a MALDI-TOFMS analysis demonstrated that the molecular mass of the mild-AGE-BSA was 658 Da larger than the native BSA (Fig. 1B), indicating that our experimentally prepared mild-AGE-BSA is already more profoundly modified than physiological human serum albumin under (patho)physiological conditions. Furthermore, although only ~3% of lysine residues of HSA were modified in dialysis patient [15], >49% lysine-modification is required to be a ligand for the scavenger receptor (Fig. 4). Taken together, our results demonstrate that the endocytic uptake of physiologically generated AGE-proteins through scavenger receptors is either negligible or unlikely to occur *in vivo*, and that AGEs detected inside foam cells in atherosclerotic lesions are generated intracellularly rather than representing the endocytic uptake of extracellular AGE-proteins by the scavenger receptors. Although most other researchers prepare the AGE-proteins with unphysiologically high concentrations of aldehydes and then are employed for the cellular experiments, some researchers consider the issues and have also prepared AGE-proteins with physiologically relevant concentrations of glycating agents in order to perform cellular experiments. For instance, macrophage-colony stimulating factor (M-CSF) is released from mature human monocytes and human monocytic THP-1 cells by incubating with HSA minimally-modified by methylglyoxal (MG_{min}-HSA) and glucose (AGE_{min}-HSA) [27]. MG_{min}-HSA also induces the synthesis and secretion of tumor necrosis factor-α (TNF-α) from human monocytic THP-1 cells in vitro [28]. Furthermore, Xu et al. [29] demonstrated that mildly-modified AGE-BSA which was prepared by incubating 50 mM glucose inhibits nitric oxide synthesis of human endothelial cells, indicating that several cellular interactions take place even AGE-proteins with physiologically relevant concentrations of glycating agents. These results suggest that mildly modified AGE-proteins may be recognized by AGE receptors such as RAGE and induce several cellular responses *in vivo*. This study demonstrates the first evidence that the ligand activity of the AGE-proteins to the scavenger receptors is dependent on their rate of modification by the AGEs, and we should carefully prepare the AGE-proteins *in vitro* to clarify the physiological significance of the interaction between the AGE-receptors and AGE-proteins.

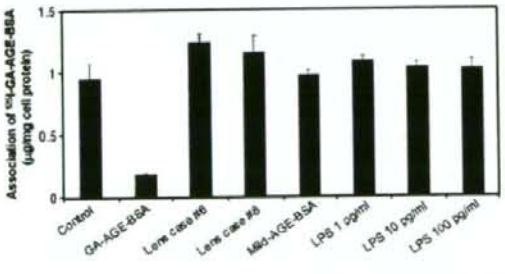

Fig. 5. Inhibitory effect of human lens proteins on the association of GA-AGE-BSA to RAW 264.7 cells. RAW 264.7 cells were incubated at 37 °C for 6 h with 2 μg/ml of ^{125}I-AGE-GA-BSA (82.5% of lysine residues were modified) in the presence of 50-fold unlabeled diabetic human lens samples, GA-AGE-BSA or mild-AGE-BSA. LPS was also used at 1–100 pg/ml. The CML content of diabetic lens samples case #6 and #8 were 19.6 and 16.8 mmol CML/mol Lys, respectively. Amounts of cell-associated ^{125}I-AGE-GA-BSA were determined as described in Materials and methods. Data are mean±SD, $n=2$.

Acknowledgments

This work was supported in part by a Grant-in-Aid for scientific Research (No. 18790619 to Ryoji Nagai) from the Ministry of Education, Science, Sports and Cultures of Japan.

References

[1] T. Higashi, H. Sano, T. Saishoji, K. Ikeda, Y. Jinnouchi, T. Kanzaki, N. Morisaki, H. Rauvala, M. Shichiri, S. Horiuchi, The receptor for advanced glycation end products mediates the chemotaxis of rabbit smooth muscle cells, Diabetes 46 (1997) 463–472.

[2] Y. Jinnouchi, H. Sano, R. Nagai, H. Hakamata, T. Kodama, H. Suzuki, M. Yoshida, S. Ueda, S. Horiuchi, Glycolaldehyde-modified low density lipoprotein leads macrophages to foam cells via the macrophage scavenger receptor, J. Biochem. (Tokyo) 123 (1998) 1208–1217.

[3] R. Nagai, K. Matsumoto, X. Ling, H. Suzuki, T. Araki, S. Horiuchi, Glycolaldehyde, a reactive intermediate for advanced glycation end products, plays an important role in the generation of an active ligand for the macrophage scavenger receptor, Diabetes 49 (2000) 1714–1723.

[4] H. Suzuki, Y. Kurihara, M. Takeya, N. Kamada, M. Kataoka, K. Jishage, O. Ueda, H. Sakaguchi, T. Higashi, T. Suzuki, Y. Takashima, Y. Kawabe, O. Cynshi, Y. Wada, M. Honda, H. Kurihara, H. Aburatani, T. Doi, A. Matsumoto, S. Azuma, T. Noda, Y. Toyoda, H. Itakura, Y. Yazaki, T. Kodama, et al., A role for macrophage scavenger receptors in atherosclerosis and susceptibility to infection, Nature 386 (1997) 292–296.

[5] N. Ohgami, R. Nagai, M. Ikemoto, H. Arai, A. Kuniyasu, S. Horiuchi, H. Nakayama, Cd36, a member of the class b scavenger receptor family, as a receptor for advanced glycation end products, J. Biol. Chem. 276 (2001) 3195–3202.

[6] N. Ohgami, R. Nagai, A. Miyazaki, M. Ikemoto, H. Arai, S. Horiuchi, H. Nakayama, Scavenger receptor class B type I-mediated reverse cholesterol transport is inhibited by advanced glycation end products, J. Biol. Chem. 276 (2001) 13348–13355.

[7] T. Jono, A. Miyazaki, R. Nagai, T. Sawamura, T. Kitamura, S. Horiuchi, Lectin-like oxidized low density lipoprotein receptor-1 (LOX-1) serves as an endothelial receptor for advanced glycation end products (AGE), FEBS Lett. 511 (2002) 170–174.

[8] A.M. Schmidt, M. Vianna, M. Gerlach, J. Brett, J. Ryan, J. Kao, C. Esposito, H. Hegarty, W. Hurley, M. Clauss, et al., Isolation and characterization of two binding proteins for advanced glycosylation end products from bovine lung which are present on the endothelial cell surface, J. Biol. Chem. 267 (1992) 14987–14997.

[9] A.M. Schmidt, O. Hori, J.X. Chen, J.F. Li, J. Crandall, J. Zhang, R. Cao, S.D. Yan, J. Brett, D. Stern, Advanced glycation endproducts interacting with their endothelial receptor induce expression of vascular cell adhesion molecule-1 (VCAM-1) in cultured human endothelial cells and in mice. A potential mechanism for the accelerated vasculopathy of diabetes, J. Clin. Invest. 96 (1995) 1395–1403.

[10] K. Ichikawa, M. Yoshinari, M. Iwase, M. Wakisaka, Y. Doi, K. Iino, M. Yamamoto, M. Fujishima, Advanced glycosylation end products induced tissue factor expression in human monocyte-like U937 cells and increased tissue factor expression in monocytes from diabetic patients, Atherosclerosis 136 (1998) 281–287.

[11] H. Vlassara, H. Fuh, Z. Makita, S. Krungkrai, A. Cerami, R. Bucala, Exogenous advanced glycosylation end products induce complex vascular dysfunction in normal animals: a model for diabetic and aging complications, Proc. Natl. Acad. Sci. U. S. A. 89 (1992) 12043–12047.

[12] W. Cai, J.C. He, L. Zhu, C. Lu, H. Vlassara, Advanced glycation end product (AGE) receptor 1 suppresses cell oxidant stress and activation signaling via EGF receptor, Proc. Natl. Acad. Sci. U. S. A. 103 (2006) 13801–13806.

[13] M. Takeuchi, S. Yamagishi, Alternative routes for the formation of glyceraldehyde-derived AGEs (TAGE) in vivo, Med. Hypotheses 63 (2004) 453–455.

[14] R. Nagai, Y. Unno, M.C. Hayashi, S. Masuda, F. Hayase, N. Kinae, S. Horiuchi, Peroxynitrite induces formation of N(epsilon)-(carboxymethyl) lysine by the cleavage of Amadori product and generation of glucosone and glyoxal from glucose: novel pathways for protein modification by peroxynitrite, Diabetes 51 (2002) 2833–2839.

[15] P.J. Thornalley, M. Argirova, N. Ahmed, V.M. Mann, O. Argirov, A. Dawnay, Mass spectrometric monitoring of albumin in uremia, Kidney Int. 58 (2000) 2228–2234.

[16] W. Koito, T. Araki, S. Horiuchi, R. Nagai, Conventional antibody against Nepsilon-(carboxymethyl)lysine (CML) shows cross-reaction to Nepsilon-(carboxyethyl)lysine (CEL): immunochemical quantification of CML with a specific antibody, J. Biochem. (Tokyo) 136 (2004) 831–837.

[17] K. Fukuhara-Takaki, M. Sakai, Y. Sakamoto, M. Takeya, S. Horiuchi, Expression of class A scavenger receptor is enhanced by high glucose in vitro and under diabetic conditions in vivo: one mechanism for an increased rate of atherosclerosis in diabetes, J. Biol. Chem. 280 (2005) 3355–3364.

[18] D.J. Hnatowich, W.W. Latne, R.L. Childs, The preparation and labeling of DTPA-coupled albumin, Int. J. Appl. Isot. 33 (1982) 327–332.

[19] K. Yamaoka, Y. Tanigawara, T. Nakagawa, T. Uno, A pharmacokinetic analysis program (multi) for microcomputer, J. Pharmacobio-Dyn. 4 (1981) 879–885.

[20] J.A. Dunn, J.S. Patrick, S.R. Thorpe, J.W. Baynes, Oxidation of glycated proteins: age-dependent accumulation of N epsilon-(carboxymethyl)lysine in lens proteins, Biochemistry 28 (1989) 9464–9468.

[21] S. Horiuchi, Y. Sakamoto, M. Sakai, Scavenger receptors for oxidized and glycated proteins, Amino Acids 25 (2003) 283–292.

[22] B. Smedsrod, J. Melkko, N. Araki, H. Sano, S. Horiuchi, Advanced glycation end products are eliminated by scavenger-receptor-mediated endocytosis in hepatic sinusoidal Kupffer and endothelial cells, Biochem. J. 322 (Pt 2) (1997) 567–573.

[23] K. Matsumoto, H. Sano, R. Nagai, H. Suzuki, T. Kodama, M. Yoshida, S. Ueda, B. Smedsrod, S. Horiuchi, Endocytic uptake of advanced glycation end products by mouse liver sinusoidal endothelial cells is mediated by a scavenger receptor distinct from the macrophage scavenger receptor class A, Biochem. J. 352 (Pt 1) (2000) 233–240.

[24] M.X. Fu, J.R. Requena, A.J. Jenkins, T.J. Lyons, J.W. Baynes, S.R. Thorpe, The advanced glycation end product, Nepsilon-(carboxymethyl) lysine, is a product of both lipid peroxidation and glycoxidation reactions, J. Biol. Chem. 271 (1996) 9982–9986.

[25] R. Nagai, C.M. Hayashi, L. Xia, M. Takeya, S. Horiuchi, Identification in human atherosclerotic lesions of GA-pyridine, a novel structure derived from glycolaldehyde-modified proteins, J. Biol. Chem. 277 (2002) 48905–48912.

[26] H.P. Hammes, X. Du, D. Edelstein, T. Taguchi, T. Matsumura, Q. Ju, J. Lin, A. Bierhaus, P. Nawroth, D. Hannak, M. Neumaier, R. Bergfeld, I. Giardino, M. Brownlee, Benfotiamine blocks three major pathways of hyperglycemic damage and prevents experimental diabetic retinopathy, Nat. Med. 9 (2003) 294–299.

[27] E.A. Abordo, M.E. Westwood, P.J. Thornalley, Synthesis and secretion of macrophage colony stimulating factor by mature human monocytes and human monocytic THP-1 cells induced by human serum albumin derivatives modified with methylglyoxal and glucose-derived advanced glycation endproducts, Immunol. Lett. 53 (1996) 7–13.

[28] E.A. Abordo, P.J. Thornalley, Synthesis and secretion of tumour necrosis factor-alpha by human monocytic THP-1 cells and chemotaxis induced by human serum albumin derivatives modified with methylglyoxal and glucose-derived advanced glycation endproducts, Immunol. Lett. 58 (1997) 139–147.

[29] B. Xu, Y. Ji, K. Yao, Y.X. Cao, A. Ferro, Inhibition of human endothelial cell nitric oxide synthesis by advanced glycation end-products but not glucose: relevance to diabetes, Clin. Sci. (Lond) 109 (2005) 439–446.

Cystathionine β-Synthase as a Carbon Monoxide–Sensitive Regulator of Bile Excretion

Tsunehiro Shintani,* Takuya Iwabuchi,* Tomoyoshi Soga, Yuichiro Kato, Takehiro Yamamoto, Naoharu Takano, Takako Hishiki, Yuki Ueno, Satsuki Ikeda, Tadayuki Sakuragawa, Kazuo Ishikawa, Nobuhito Goda, Yuko Kitagawa, Mayumi Kajimura, Kenji Matsumoto, and Makoto Suematsu

Carbon monoxide (CO) is a stress-inducible gas generated by heme oxygenase (HO) eliciting adaptive responses against toxicants; however, mechanisms for its reception remain unknown. Serendipitous observation in metabolome analysis in CO-overproducing livers suggested roles of cystathionine β-synthase (CBS) that rate-limits transsulfuration pathway and H_2S generation, for the gas-responsive receptor. Studies using recombinant CBS indicated that CO binds to the prosthetic heme, stabilizing 6-coordinated CO-Fe(II)-histidine complex to block the activity, whereas nitric oxide (NO) forms 5-coordinated structure without inhibiting it. The CO-overproducing livers down-regulated H_2S to stimulate HCO_3^--dependent choleresis: these responses were attenuated by blocking HO or by donating H_2S. Livers of heterozygous CBS knockout mice neither down-regulated H_2S nor exhibited the choleresis while overproducing CO. In the mouse model of estradiol-induced cholestasis, CO overproduction by inducing HO-1 significantly improved the bile output through stimulating HCO_3^- excretion; such a choleretic response did not occur in the knockout mice. *Conclusion:* Results collected from metabolome analyses suggested that CBS serves as a CO-sensitive modulator of H_2S to support biliary excretion, shedding light on a putative role of the enzyme for stress-elicited adaptive response against bile-dependent detoxification processes. (HEPATOLOGY 2009;49:141-150.)

Carbon monoxide (CO) is generated from inducible heme oxygenase 1 (HO-1) and constitutive heme oxygenase 2 (HO-2), respectively, and has the ability to regulate neurovascular functions,[1,2] apoptotic responses,[3,4] and metabolism of xenobiotics and toxicants.[5,6] This gas is overproduced through increased delivery of heme as a substrate and the HO-1 induction on exposure to stressors such as hypoxia and oxidative stress. Mechanisms by which CO regulates cell functions appear to involve an activation of soluble guanylate cyclase (sGC), the enzyme that allows the gas to bind to the prosthetic heme to synthesize cyclic guanosine monophosphate as a second messenger.[1] Distinct from nitric oxide (NO) that forms 5-coordinated NO-Fe(II) complex to trigger full activation of the enzyme, CO activates this enzyme only modestly because the gas binding stabilizes 6-coordinated CO-Fe(II)-histidine complex.[7] Mitogen-activated protein kinase has also been shown to serve as a CO-responsive signal transducer.[8] Gene disruption of HO-1 increases sensitivity to overproduction of reactive oxygen species, inflammatory mediators or xenobiotic metabolism, whereas the gene transfer or CO inhalation under these circumstances suppresses such pathogenic responses.[7-9] However, direct mechanisms for the CO reception to trigger these adaptive responses of metabolism remain unknown.

Because this gas has the ability to inhibit ferrous form of the prosthetic heme of enzymes, tryptophan 2,3-dioxygenase or cytochromes P450 have been considered puta-

Abbreviations: CBS, cystathionine β-synthase; CE-MS, capillary electrophoresis equipped with mass spectrometry; CO, carbon monoxide; CORM, CO-releasing metal carbonyl tricarbonyldichlororuthenium (II); ES, 17α-ethinylestradiol; GSH, glutathione; GSNO, S-nitrosyl glutathione; H12, liver exposed to 12-hour hemin treatment; NO, nitric oxide; $RuCl_3$, CO-free ruthenium (III) chloride; SAM, S-adenosyl methionine; SE, standard error; sGC, soluble guanylate cyclase.

From the Department of Biochemistry and Integrative Medical Biology, Department of Surgery, School of Medicine, Keio University, Tokyo, Japan; the Institute for Advanced Biosciences, Keio University, Tsuruoka City, Japan; and the First Department of Surgery, College of Medicine, Nagoya University, Nagoya, Japan.

Received July 3, 2008; accepted August 25, 2008.

**These authors contributed equally to this work.*

T.H. is a postdoctoral research fellow supported by Grant-in-Aid for Creative Scientific Research 17GS0419 from JSPS in Japan. Development of the methodology for differential metabolomic analyses using contrast-enhanced time of flight/mass spectrometry was supported by Leading Project for Biosimulation from MEXT. T.I. and T.Y. are research associates of Global COE Program for Metabolomic Systems Biology from MEXT and MHLW.

Address reprint requests to: Makoto Suematsu, M.D., Ph.D., Professor and Chair, Department of Biochemistry and Integrative Medical Biology, School of Medicine, Keio University, 35 Shinanomachi, Shinjuku-ku, Tokyo 160-8582, Japan. E-mail: msuem@sc.itc.keio.ac.jp; fax: (81)-3-5363-3466.

Published online in Wiley InterScience (www.interscience.wiley.com).

DOI 10.1002/hep.22604

Potential conflict of interest: Nothing to report.

tive CO-sensitive signal transducers regulating cell functions, including cell proliferation,[10] immune responses,[11] microvascular tone, xenobiotic detoxification, and biliary excretion in the liver.[5,6,12] However, ferrous heme of these enzymes is not only sensitive to CO but to NO. In this context, whether mechanisms by which CO regulates cell and organ functions is not shared by those for NO has not fully been studied yet.

This study aimed to mine novel CO-responsive regulators for stress-inducible adaptation of metabolism. To this end, we have used metabolome analyses based on capillary electrophoresis equipped with mass spectrometry (CE-MS) for systematic mining CO-responsive gaseous signal transducers. The current results suggest that cystathionine β-synthase (CBS), the enzyme rate-limiting transsulfuration pathway is such a novel CO-sensitive regulator of metabolism that plays an important role for quality control of bile excretion under disease conditions.

Materials and Methods

Preparation of Mice. The experimental protocols herein described were approved by our institutional guidelines provided by the Animal Care Committee of Keio University School of Medicine. Mice heterozygous for disruption in the CBS gene were purchased from Jackson Labs (Bar Harbor, MI) and bred at our institution. Male heterozygous CBS-deficient mice ($CBS^{+/-}$) and their littermates ($CBS^{+/+}$), and wild-type B6J mice, which were purchased from Clea Japan, Inc (Kawasaki City, Japan), were used at 8 to 12 weeks of age. Mice were allowed free access to laboratory chow and tap water, and were fasted for 18 hours before experiments. Mice were anesthetized with an intraperitoneal injection of ketamine at 120 mg/kg, and xylidine at 6 mg/kg. Their common bile ducts were ligated in proximity to the duodenum, and the gallbladder was nicked and cannulated with a polyethylene P-10 tube to collect bile for 20 minutes after a 10-minute stabilization period.[6,13] Biliary constituents such as total bile salts, bilirubin-IXα, pH values, and bicarbonate (HCO_3^-) were measured according to previous methods described elsewhere.[13] When necessary, biliary samples were collected into tubes containing 10% trichloroacetate to measure glutathione through high-performance liquid chromatography.[14] Determination of bilirubin-IXα in bile serves as an indicator of HO-mediated heme degradation in the liver that occurs in parallel with endogenous CO generation. Hepatic CO contents were also measured by gas chromatography as described previously,[15] except that the flame ionization detector equipped with a methanizer was used in this study instead of a reduction gas detector. Combination of these methods to determine CO allowed us to distinguish endogenous CO generation from the same gas exogenously administered as an intervention as described in the following session.

Administration of Reagents Studied. Protoheme IX (hemin) was administered at 40 μmol/kg intraperitoneally at 12 hours before surgical preparation for bile collection. This protocol was denoted as liver exposed to 12-hour hemin treatment (H12) treatment in the text. After collecting bile, livers were excised immediately to be snap-frozen in cold methanol, and the lysates served as samples for contrast-enhanced time of flight/mass spectrometry analyses as described later. In separate sets of experiments, liver samples were minced with 10% trichloroacetic acid at 4°C to measure cysteine and glutathione (GSH) through high-performance liquid chromatography to confirm the data collected from contrast-enhanced time of flight/mass spectrometry, when necessary.

A series of protocols were employed to examine roles of HO-derived CO in regulation of H_2S-modulated choleresis in the H12-treated mice. First, zinc protoporphyrin, a potent HO inhibitor, was administered intravenously at 12.5 μmol/hour/kg at 30 minutes before the bile collection; this dose was sufficient to block endogenous CO in the liver. When necessary, tricarbonyldichlororuthenium (II) dimer, the CO-releasing metal carbonyl [tricarbonyldichlororuthenium (II): CORM, Sigma-Aldorich][16] was administered intraportally at 30 minutes before the start of bile collection. When necessary, CO-free ruthenium (III) chloride ($RuCl_3$) was used as a negative control reagent. To examine whether the elevation of H_2S in the liver could alter biliary HCO_3^- excretion, sodium hydrosulfide (NaHS) was administered at 20 μmol/hour/kg through the portal vein at 30 minutes before the bile collection; as seen later in Results, this protocol restored the H12-induced decrease in the hepatic H_2S contents without altering a reduction of systemic blood pressure that was induced by a systemic bolus of the NaHS injection. S-nitrosyl glutathione (GSNO) was used as an NO donor. The reagent was injected intraportally with a dose of 7 μmol/kg at 30 minutes before the collection of bile; this protocol did not induce a reduction of systemic blood pressure, whereas greater doses caused hypotension and subsequent decrease in the bile output. In these experiments, administration of the reagent was performed through a 30-gauge miniature needle that was inserted into the portal vein to be fixed at the site of puncture. Finally, to examine therapeutic effects of CO, we examined effects of H12 treatment or administration of CORM in the mice exposed to drug-induced cholestasis. To this end, cholestasis was induced by a subcutane-

ous injection of 17α-ethinylestradiol (ES) at 5 mg/kg daily for 5 consecutive days before the experiments.[17]

Metabolome Analysis. We performed metabolome analyses of tissue lysates collected from snap-frozen livers of mice using contrast-enhanced time of flight/mass spectrometry according to our previous methods.[18,19] Measurements of hepatic H_2S contents were based on gas chromatography described in our previous method.[14] Biliary flux of bilirubin-IXα (BR-IXα) in bile samples were determined by enzyme-linked immunosorbent assay using the anti–BR-IXα monoclonal antibody as described previously.[6,20] Because BR-IXα is an end product of the HO-mediated degradation of protoheme IX, its measurements in bile serves as an index of endogenous CO generation in the liver.[20] The conversion of ^{15}N-methionine to its downstream metabolites was determined by CE-MS to examine different rates of the metabolic flux through CBS in the liver. In these experiments, ^{15}N-methionine was intraperitoneally injected at 150 μmol/100 g body weight, and ^{15}N-homocysteine and ^{15}N-cystathionine were measured by CE-MS using the lysates of liver tissues at 30, 60, and 120 minutes after the methionine challenge. Data were expressed as percentages of the mass-labeled metabolites versus total amounts of metabolites in remethylation cycle [ΣRM: methionine + S-adenosyl methionine (SAM) + S-adenosyl homocysteine (SAH) + homocysteine]. In a separate set of experiments, effects of application of CO on contents of methionine and cystathionine in HepG2 cells were determined in culture. In these experiments, the cells were maintained in Roswell Park Memorial Institute 1640 medium (Invitrogen, Carlsbad, CA) containing 10% fetal bovine serum; the mixture was supplemented with 1× penicillin/streptomycin and maintained at 37°C in an atmosphere of 5% CO_2/95% air. The cells were treated with either 50 μmol/L CORM or $RuCl_3$ as a negative control for 16 hours. To measure the metabolites, a frozen pellet of the 1×10^6 cells was homogenized in 10% trichloroacetic acid with 10 mM diethylene triamine pentaacetic acid following brief centrifugation, and the supernatant was used as a sample.

Western Blot Analysis. Western blot analysis was carried out to examine an induction of heme oxygenase (HO)-1 using the polyclonal antibody SPA896 (Stressgen, Ann Arbor, MI). In these experiments, the blotting against α-tubulin was carried out using the polyclonal antibody (Cell Signaling, Danvers, MA) as an internal control.

Recombinant Full-Length Rat CBS. The complementary DNA of the full-length rat CBS was a gift from Professor Masao Ikeda-Saito in Tohoku University. Stopped-flow equipment was purchased from Unisoku, Inc. (Tokyo) and used to examine binding of CO or NO to the CBS protein according to previous methods.[21] Electron paramagnetic resonance spectrometry to determine 5-coordinated structure of the nitrosylheme complex of CBS was carried out according to previous methods.[21,22]

Statistical Analyses. The statistical significance of data among different experimental groups was determined by one-way analysis of variance and Fischer's multiple comparison test. $P < 0.05$ was considered significant.

Results

CO Overproduction Inhibits Transsulfuration and H_2S and Stimulates HCO_3^- Choleresis. Metabolome analyses based on CE-MS allowed us to pinpoint metabolic pathways responding to disease conditions. In mouse liver, we detected more than 1800 metabolites, and compared differences between the control and acetaminophen-treated livers.[18] This method was used to determine differences in metabolic responses between mouse livers and those overloaded with heme, the stressor inducing oxidative stress and subsequent CO overproduction through increasing the substrate and inducing HO-1 (Fig. 1A). The hepatic CO flux peaked at 6 hours, becoming threefold to fourfold greater during the 6 to 12 hours after challenging with hemin, as judged by BR-IXα, an end product of HO-mediated heme degradation (Fig. 1B).[13] Under these conditions, bile output was modestly but significantly increased at 12 to 18 hours after the treatment (Fig. 1C) in parallel with significant elevation of HCO_3^- to make bile more alkaline (Fig. 1D-F), enhancing solubility of organic anions during the detoxification processes. These results suggest that the heme-elicited choleretic response is not correlated with vasodilatory mechanisms by the gas. Based on these results, we used CE-MS analyses to examine metabolomics in the liver exposed to 12-hour hemin treatment (H12), in which phenotypes of bile remodeling became evident.

Among known metabolites (Table 1), most prominent differences between the control and H12 groups occurred in global decreases in amino acids concurrent with increases in Krebs cycle substrates such as acetyl CoA: the fact that these changes coincided with sustained glutamate, significant increases in glutamine, and high-energy adenosine phosphates appeared to suggest utilization of the amino acid pool for energy substrates. By contrast, several essential amino acids such as methionine, tryptophan and histidine, and serine were maintained. Another important alteration was a global decrease in transsulfuration metabolites such as cystathionine, cysteine, and

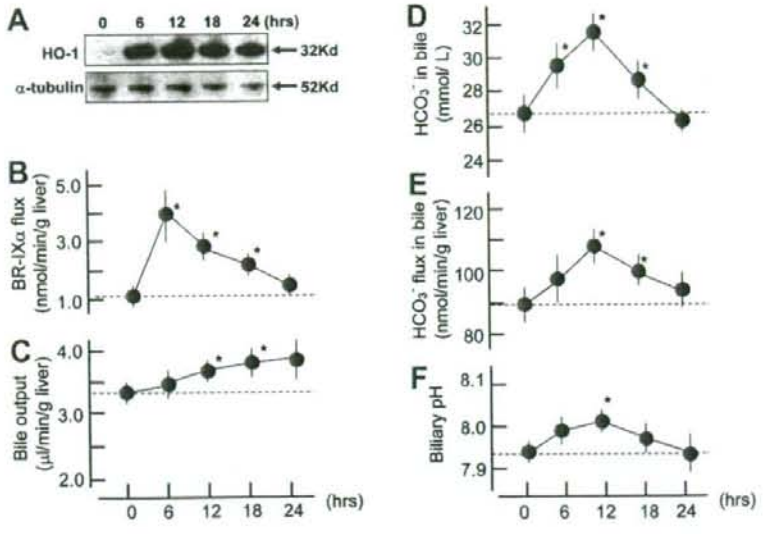

Fig. 1. Temporal alterations in hepatic generation of CO and biliary function after overloading heme. (A) Western blots indicating the induction of heme oxygenase (HO)-1. Alpha-tubulin is an internal control. (B) Biliary excretion of bilirubin-IXα (BR-IXα), a terminal metabolite of HO-dependent heme degradation, as an index of endogenous CO generation through heme oxygenase in the liver. (C) Bile output. (D) Biliary concentration of HCO_3^-. (E) Biliary flux of HCO_3^-. (F) pH values of bile. $^*P < 0.05$ versus the value measured at time 0, which is before the intraperitoneal hemin administration at 40 μmol/kg.

hypotaurine. These results led us to determine tissue contents of H_2S, the terminal product derived from CBS or cystathionine γ-lyase that constitute transsulfuration pathway; this gaseous compound turned out to be suppressed in the H12 group. Based on these measurements, we hypothesized that the H12 treatment limits the activity of CBS so far as judged from maintenance of methionine pool (ΣRM) and serine, a substrate of the enzyme, with suppression of the transsulfuration metabolites residing in the downstream (Fig. 2A). This hypothesis was confirmed by in vivo pulse-chase analysis showing accumulation of ^{15}N-homocysteine and suppression of ^{15}N-cystathionine after the ^{15}N-methionine challenge in the H12 group (Fig. 2B).

Such an inhibitory action of the H12 treatment on the transsulfuration pathway was reproducible when HepG2 cells was treated with CO in culture; contents of cystathionine were significantly suppressed by the application of 50 μmol/L CORM (9.3 ± 1.3 versus 15.9 ± 1.4 nmol/g protein for the vehicle treatment with $RuCl_3$. Mean ± standard error (SE) of three separate experiments, $P < 0.03$), whereas methionine exhibited no difference (66.3 ± 3.7 versus 80.3 ± 12.2 nmol/g protein for CORM and $RuCl_3$, respectively. Mean ± SE of three separate experiments), suggesting inhibitory action of the gas on CBS.

CO But Not NO Inhibits CBS. H12-induced metabolomic changes indicating dissociation between remethylation cycle and transsulfuration pathway led us to hypothesize that CBS, a heme-containing enzyme that rate-limits the transsulfuration pathway, is a sensor of the H12-elicited CO overproduction. Rat full-length recombinant CBS were purified (Fig. 3A) to examine whether CO or NO could inhibit the enzyme activities. CO, but not NO, specifically inhibited the enzyme (Fig. 3B). Previous crystallographic studies using a truncated form of CBS showed that the axial ligands for the prosthetic heme were cysteine and histidine, indicating a large peak of absorbance at 448 nm.[23] On CO application, the heme formed a 6-coordinated CO-Fe(II)–histidine complex, as judged by a decrease in the absorbance at 448 nm and a reciprocal elevation at 422 nm (Fig. 3C). These results were consistent with previous works using the truncated form of human recombinant CBS.[24] Such an inhibitory effect of CO on CBS activity occurred even when sufficient amounts of SAM were present as an allosteric activator,[25] whereas the CO concentrations necessary to suppress CBS became greater in the presence of SAM (Fig. 3D). Conversely, NO was able to bind to the heme but with a distinct structure of 5-coordinated nitrosyl-heme as judged by electron paramagnetic resonance spectrometry (Fig. 3E), suggesting that the enzyme responds specifically to the binding of CO but not that of NO.

CO-Induced HCO_3^- Choleresis Is Sensitive to H_2S and Disappears in CBS$^{+/-}$ Mice. Recent studies indicated that H_2S derived from cystathionine γ-lyase, an enzyme using cysteine to generate the gas, modulates biliary HCO_3^- excretion via mechanisms involving glibenclamide-sensitive channels, a putative H_2S target.[14,26] We hypothesized that the stress-induced CO stimulates the HCO_3^- excretion to increase pH in bile through its inhibitory action on CBS-derived H_2S. To examine this hypothesis, we chose the dose of the CO-releasing molecule (CORM) that was able to increase hepatic contents

Table 1. Comparison of Metabolome Analysis by CE-MS in Liver Extracts Between Control and the Hemin-Treated (H12) Mice

	Control	H12
Carbohydrates (nmol/g liver)		
Glucose 1-P	20 ± 4	31 ± 5
Glucose 6-P	24 ± 1	22 ± 6
Ribulose 5-P	206 ± 60	115 ± 17
Fructose 6-P	25 ± 1	21 ± 6
Glycerol 3-P	1800 ± 250	1663 ± 218
Lactate	3490 ± 633	2920 ± 385
Acetyl CoA	3.4 ± 0.5	6.2 ± 1.1*
Malonyl CoA	37 ± 6	83 ± 15*
Citrate	70 ± 13	88 ± 20
Fumarate	120 ± 22	167 ± 52
Malate	343 ± 91	479 ± 90
CoA	132 ± 21	111 ± 20
Nucleotides (nmol/g liver)		
ATP	208 ± 35	480 ± 90*
GTP	33 ± 4	79 ± 14*
ADP	577 ± 104	1060 ± 154*
AMP	1866 ± 277	1863 ± 70
IMP	501 ± 82	660 ± 99
Adenosine	203 ± 18	151 ± 11
Adenine	12 ± 1	12 ± 2
Hypoxanthine	58 ± 8	43 ± 15
	Control	**H12**
Amino acids (μmol/g liver)		
Gly	3.16 ± 0.11	2.20 ± 0.05*
Ala	3.12 ± 0.48	1.47 ± 0.40*
Ser	0.38 ± 0.07	0.31 ± 0.05
Pro	0.37 ± 0.03	0.27 ± 0.04*
Val	0.41 ± 0.01	0.23 ± 0.05*
Thr	0.31 ± 0.03	0.20 ± 0.04*
Lys	0.69 ± 0.13	0.46 ± 0.05*
Cys	0.20 ± 0.04	0.07 ± 0.03*
Leu	0.36 ± 0.02	0.25 ± 0.05†
Asp	0.76 ± 0.13	0.59 ± 0.12†
Glu	2.90 ± 0.16	2.75 ± 0.28
Gln	3.39 ± 0.58	6.48 ± 0.54*
His	0.43 ± 0.05	0.48 ± 0.02
Amino acids and derivatives (nmol/g liver)		
Met	49 ± 5	39 ± 10
GABA	29 ± 2	25 ± 4
Ornithine	420 ± 95	226 ± 22*
Asn	77 ± 7	59 ± 3*
Ile	175 ± 12	94 ± 17*
Arg	8.8 ± 1.2	4.8 ± 0.6*
Citrulline	64 ± 10	35 ± 3*
Trp	34 ± 2	31 ± 3
Tyr	111 ± 15	52 ± 8*
Glu-2 aminobutyrate	6.3 ± 2.3	5.7 ± 1.2
Ophthalmate	67 ± 7	83 ± 6

Data indicate mean ± SE of six separate experiments.

Data of metabolites in remethylation cycle and transsulfuration pathway were indicated in Fig. 2A.

*$P < 0.05$ and †$P < 0.1$ versus controls.

of CO comparably to those measured in the H12 treatment: As seen (Fig. 4A), the intraportal administration of CORM at 20 μmol/kg significantly increased hepatic CO contents comparable to those induced by H12 treatment in the intact mice. This dose of CORM suppressed hepatic H_2S and stimulated biliary HCO_3^- flux. Stimulatory effects of CO administration on biliary HCO_3^- excretion in intact mice were not shared by NO, as judged by observation in the mice administered with GSNO, an NO donor (Fig. 4B): These results were consistent with observation that CBS is sensitive to CO but not to NO in vitro (Fig. 3).

As already seen, H12 treatment increased CO generation (biliary BR-IXα flux), decreased hepatic H_2S contents, and stimulated biliary HCO_3^- flux (Fig. 1). HO blockade by zinc protoporphyrin-IX cancelled these changes elicited by H12 treatment. On the other hand, an administration of NaHS, an H_2S donor, abolished the H12-induced suppression of hepatic H_2S contents, and significantly attenuated the stimulatory response of biliary HCO_3^- flux (Fig. 5A), suggesting that H12-inducible CO stimulates biliary HCO_3^- excretion through modulation of CBS-derived H_2S. As previously reported, homozygous CBS knockout mice died of severe hepatic steatosis, whereas heterozygous knockout ($CBS^{+/-}$) mice survive through compensation without apparent phenotypes.[27] In these mice, indeed, the baseline H_2S content in livers of $CBS^{+/-}$ mice was comparable to that of $CBS^{+/+}$ mice, presumably because of compensation of the gas generation through cystathionine γ-lyase. On H12 treatment, $CBS^{+/-}$ mice exhibited an increase in the hepatic CO generation comparably to $CBS^{+/+}$ mice, but neither decreased H_2S contents nor up-regulated biliary HCO_3^- flux (Fig. 5B), indicating phenotypes distinct from those in $CBS^{+/+}$ littermates.

CO Protects Against Drug-Induced Cholestasis Through Mechanisms Involving CBS. We further attempted to investigate whether the administration of CO could improve biliary dysfunction occurring in disease models. To examine this, the mice were treated with ES, a cholestatic reagent suppressing three major osmolites such as HCO_3^-, glutathione, and bile salts in bile.[17] H12 treatment or the administration of CORM significantly increased bile output concurrently with a recovery of HCO_3^- excretion into bile (Fig. 6A). The anti-cholestatic effects of H12 treatment through stimulation of HCO_3^- excretion disappeared in the $CBS^{+/-}$ mice (Fig. 6B), suggesting again a pivotal role of CBS for triggering the CO-induced choleresis.

Discussion

CO administration or HO-1 induction has been shown to protect against tissue injury and considered a potentially useful therapeutic stratagem.[8,16] Serendipitous observation in the liver indicating effects of overproduced CO on metabolism of sulfur-containing amino

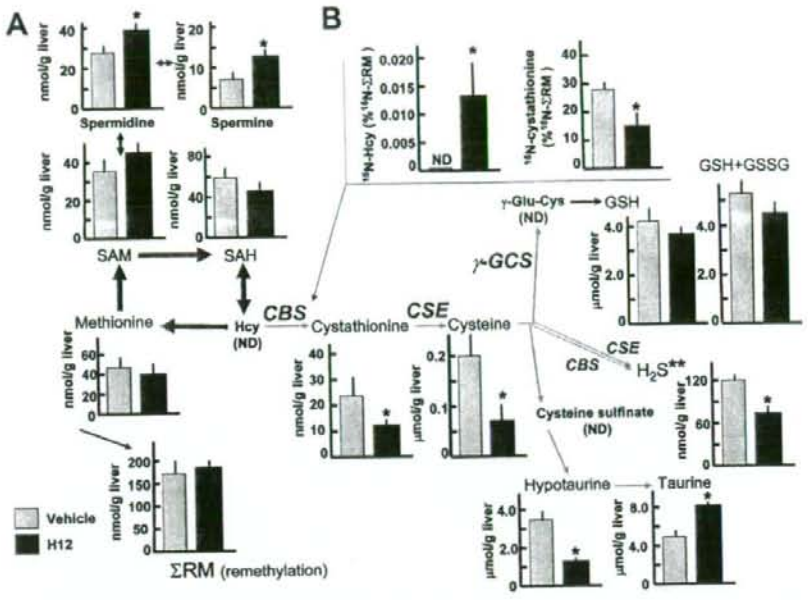

Fig. 2. Metabolomic comparison of sulfur-containing amino acids and their derivatives between the heme-overloaded and vehicle-treated livers of mice. (A) Differences in hepatic contents of the metabolites between the control and hemin-treated mice. H12: treatment with hemin at 12 hours before sampling the liver. Note decreases in transsulfuration metabolites. (B) *In vivo* pulse-chase analysis indicating conversion rates of ^{15}N-methionine into ^{15}N-homocysteine (Hcy) and ^{15}N-cystathionine in livers between the groups. The amounts of the downstream metabolites were measured at 30 minutes after the methionine administration. The data in B were normalized by total amounts of metabolites in remethylation cycle (^{15}N-methionine + ^{15}N-SAM + ^{15}N-SAH + ^{15}N-Hcy = ΣRM) at 30 minutes. ND, not detected. Data indicate mean ± SE of six to eight separate experiments for each group. *$P < 0.05$ versus the vehicle-treated group.

acids led us to reveal unique physiological actions of this gas on CBS *in vivo* that are not shared with NO. The current study suggested that stress-inducible CO targets CBS and thereby reduces H_2S significantly to stimulate biliary HCO_3^- excretion that could benefit detoxification processes. Conversely, such a property of stress-inducible CO might jeopardize anti-oxidative defense systems through an overflow of homocysteine or through a shortage of GSH. Under current experimental conditions, however, such a risk seemed little, if any, so far as judged from maintenance of GSH and adenosine triphosphate so far. This appears to result from large difference in amino acid pools between methionine (nmol/g) and thiols including cysteine and GSH (μmol/g). Furthermore, cysteine could be supplied through its uptake from extracellular space by mechanisms involving Nrf2, the transcriptional factor activated in response to oxidative stress or electrophiles such as heme.[28,29] By contrast, the amounts of sulfur-containing amino acids consumed to generate H_2S seems relatively smaller than that for synthesizing GSH or hypotaurine, as judged from quantitative information collected by metabolome analysis. Because CBS not only limits synthesis of cystathionine from homocysteine but also directly suppresses H_2S generation from cysteine, the inhibitory effects of CO on the enzyme could dictate largely on the action of H_2S in the liver, causing a stimulatory effect on bile excretion. Considering recent studies suggesting vasodilatory effects of H_2S,[26,30] suppression of CBS-derived H_2S by stress-inducible CO might trigger vasoconstriction, but such vasoactive responses did not occur so far as judged from choleretic response of the basal bile flow that is highly dictated by microvascular perfusion. This might result from the fact that stress-inducible CO itself has the ability to maintain the basal microvascular perfusion through multiple vasodilatory mechanisms involving activation of cyclic guanosine monophosphate and modulation of cytochrome P450–derived vasoconstrictors.[6,20,31]

Although the inhibitory action of stress-inducible CO on the transsulfuration pathway has first been shown in the heme-overloading detoxification model of mice in the current study, a similar event occurred in acetaminophen-induced acute liver injury model of mice in which CO was overproduced through degradation of cytochrome P450–derived heme.[5,18] Our previous study in rats suggested that another HO-derived product bilirubin but not CO

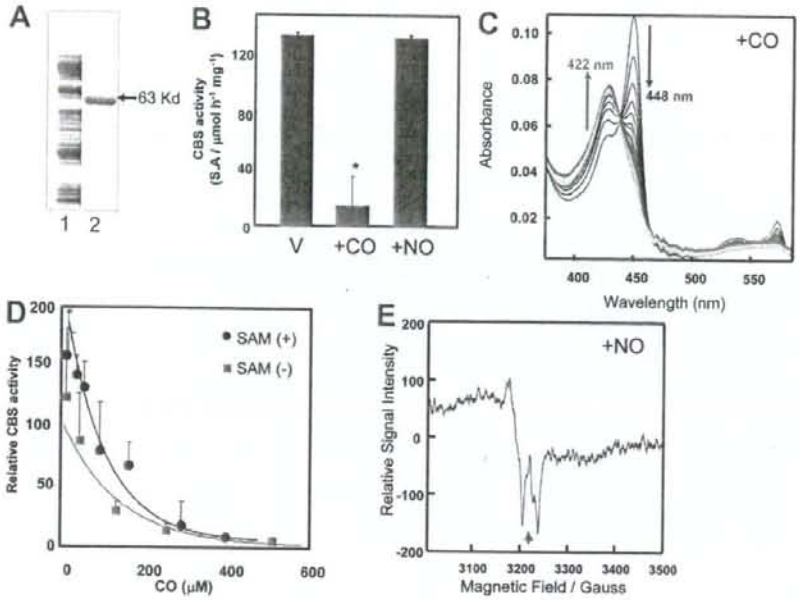

Fig. 3. Effects of CO and NO on the activity and structure of the prosthetic heme of rat recombinant full-length CBS. (A) Sodium dodecyl sulfate polyacrylamide gel electrophoresis for purification of rat recombinant CBS. Lane 1, crude extract; lane 2, purified CBS. (B) Effects of CO and NO on the Fe(II)-CBS activity under optimal substrate conditions at pH 7.4. CO but not NO (100 μM) significantly attenuated the activities of the ferrous enzyme. Data indicate mean $\pm$ SE of four experiments. The activities were measured by determining conversion of homocysteine and serine to cystathionine. $^*P < 0.05$ versus the group treated with vehicle (V). The concentration of CBS-heme was 10 μM. (C) Stopped-flow visible spectrophotometry for Fe(II)-CBS to examine temporal transitional changes after mixing with CO. Data exhibited a drop at 449 nm and a reciprocal elevation at 422 nm, demonstrating stabilization of the 6-coordinated CO-Fe(II)-histidine complex. K_{obs} = 0.638/second. (D) Effects of CO on the CBS activities in the presence or absence of S-adenosyl methionine (SAM), the allosteric activator of the enzyme. (E) Electron spin resonance spectrometry indicating 5-coordinated NO-Fe(II) complex of the CBS-heme. Arrow: g-value = 2.008.

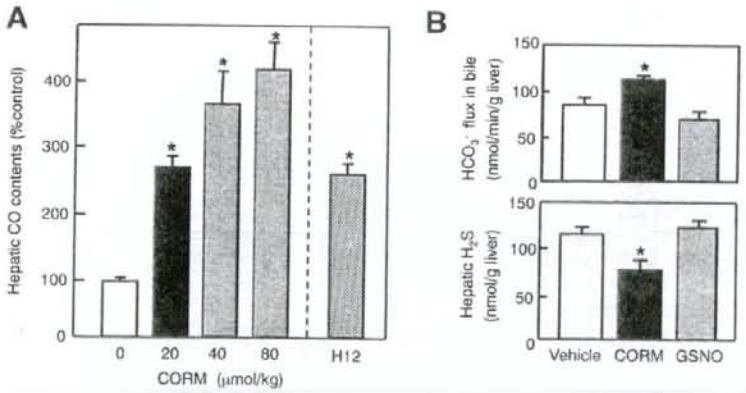

Fig. 4. Effects of the administration of CORM on hepatic CO delivery and biliary function, and their comparison with GSNO, an NO donor. (A) Effects of administration of CORM on hepatic CO contents. H12: the CO contents measured at 12 hours after an intraperitoneal injection of hemin at 40 μmol/kg. Data indicate mean $\pm$ SE of five separate experiments for each group. $^*P < 0.05$ versus the controls. Note that 20 μmol/kg CORM caused an increase comparable to that induced by H12. (B) Effects of an intraportal administration of CORM on hepatic H_2S contents and biliary HCO_3^- flux. GSNO, S-nitrosyl glutathione, an NO donor. $^*P < 0.05$ versus the values in the vehicle-treated controls. Data indicate mean $\pm$ SE of seven to eight separate experiments for each group.

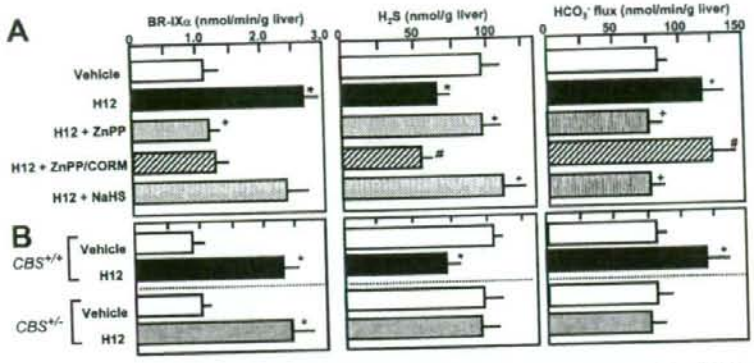

Fig. 5. Effects of HO blockade by zinc protoporphyrin and supplementation of NaHS, an H_2S donor, on biliary flux of BR-IXα, hepatic H_2S contents, and biliary HCO_3^- excretion in the 12-hour hemin-treated liver (H12). (A) Measurements in wild-type male B6 mice. Note that the hemin-induced suppression of H_2S generation and stimulation of biliary HCO_3^- excretion were sensitive to the HO inhibitor and reversed by supplementing CO (CORM). An injection of NaHS, an H_2S donor, restored hepatic H_2S contents and repressed the biliary HCO_3^- excretion in the H12-treated liver, suggesting that the biliary response is H_2S-dependent. (B) Disappearance of H12-induced reduction of H_2S and biliary HCO_3^- excretion in heterozygous CBS-knockout mice ($CBS^{+/-}$). Note that $CBS^{+/-}$ mice neither exhibit a reduction of H_2S nor up-regulate biliary HCO_3^- excretion, although overproducing CO (BR-IXα flux) comparably to the littermates ($CBS^{+/+}$). $^*P < 0.05$ versus the vehicle-treated controls. $+P < 0.05$ versus the H12-treated groups. $\#P < 0.05$ versus the H12+ zinc protoporphyrin-treated groups.

has the ability to improve bile acid–dependent bile output of the post–cold ischemic liver grafts through its antioxidative action.[32] However, such an effect of bilirubin appears to be distinct from the stimulatory action of CO on biliary fluid excretion indicated in the current study. CO has been shown to exert diverse actions on biliary function through multiple mechanisms: First, stress-inducible levels of CO have the ability to elongate the intervals of bile canalicular contraction, which helps increase the stroke volume for promoting bile excretion; this process appears to involve mechanisms mediated by modulation of cytochrome P450 epoxygenases and intra-

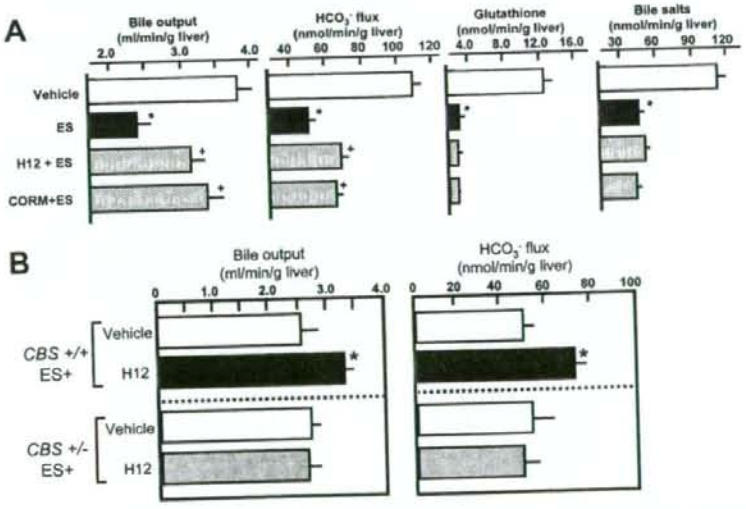

Fig. 6. Effects of H12 treatment or CORM administration on 17α-ethinylestradiol (ES)-induced cholestasis in male B6 mice. (A) Effects of H12 or CORM on ES-induced decreases in the bile output and bile constituents. ES elicited marked cholestasis, which coincided with decreases in HCO_3^-, glutathione, and bile salts in bile. Pretreatment with hemin at 12 hours before the administration of ES (H12 + ES) or the administration of CORM significantly attenuated ES-induced cholestasis through stimulation of HCO_3^- excretion into bile. (B) Effects of H12 treatment on ES-induced impairment of bile output and biliary HCO_3^- flux in $CBS^{+/+}$ and $CBS^{+/-}$ mice. $^*P < 0.05$ versus the values in vehicle-treated controls. $+P < 0.05$ versus the values in ES-treated group. Data indicate mean ± SE of eight separate experiments for each group. Note disappearance of the improving effect of H12 treatment in the $CBS^{+/-}$ mice.

cellular Ca^{2+} mobilization.[12] Second, suppression of endogenous CO activates bile acid–dependent bile excretion through accelerated vesicular transport of taurocholate, while inducing no significant elevation of the bile acid–independent fraction.[33] Conversely, CO overproduction by the HO-1 induction or exogenous administration of CO stimulates bile acid–independent choleresis concurrently with increased mrp2-dependent excretion of bilirubin-IXα and glutathione, while suppressing biliary excretion of bile salts, indicating the effects of the gas for stimulating fluid excretion into bile.[34] Of interest is that glibenclamide, an inhibitor of K^+ channel that serves as a putative target for H_2S,[26] acts on Na^+-K^+-$2Cl^-$ cotransporter in bile duct epithelium to stimulate biliary HCO_3^- excretion in normal and cholestatic livers.[35] We showed that inhibition of cystathionine γ-lyase, another H_2S-generating enzyme, stimulates basal and glibenclamide-induced fluid output of bile through stimulating HCO_3^- excretion without altering the baseline vascular resistance of the liver.[14] Recent studies provided evidence that such a glibenclamide-responsive channel is present in rodent cholangiocytes[36] or in duodenum,[37] contributing to stimulation of the HCO_3^- excretion.[36] Based on these observations, it is not unreasonable to speculate that CO stimulates biliary fluid excretion through mechanisms involving H_2S-mediated modulation of glibenclamide-sensitive channels on biliary epithelium. Although further investigation is necessary to determine whether these mechanisms are sensitive to H_2S, the current results shed light on a possibility that the CO-CBS system serves as a putative mechanism for stimulating bile acid–independent fluid excretion, facilitating excretion of HCO_3^- and organic anions such as bilirubin to support heme detoxification. Both glibenclamide and CO help biliary fluid excretion in estrogen-induced hepatocellular cholestasis. Exploration of H_2S-sensitive molecular targets occurring on biliary epithelium deserves further studies for evidence that HO-1–derived CO serves as a therapeutic stratagem for protecting against cholestasis.

CO has been believed to share varied physiological effects on biological systems with NO. However, through extrapolation of studies *in vitro* indicating biochemical actions of CO to trigger structural changes in gas-responsive heme proteins (such as sGC, hemoglobin) distinct from those elicited by NO,[7,19,21,22,38] evidence that CO is a unique gaseous regulator distinct from NO has been emerging. In fact, CO itself modestly activates sGC, by which hepatic sinusoids are constitutively dilated.[2,20,39] By contrast, in vascular smooth muscle cells in which NO is sufficiently supplied from arteriolar endothelium (for example, brain microcirculation), the inducible CO inhibits NO-elicited sGC activation.[40,41] Besides these observations suggesting physiologic actions of CO occurring dependently of local NO levels, the current study provided evidence for a novel mechanism functioning irrespective of the NO effects. Furthermore, our results shed light on a metabolic link between CO and H_2S, suggesting that different gaseous mediators constitute an intriguing link for regulation of organ functions.

Acknowledgment: The authors thank Kayo Maruyama for technical support in measuring tissue H_2S contents.

References

1. Verma A, Hirsch DJ, Glatt CE, Ronnett GV, Snyder SH. Carbon monoxide: a putative neural messenger. Science 1993;259:381-384.
2. Suematsu M, Goda N, Sano T, Kashiwagi S, Egawa T, Shinoda Y, et al. Carbon monoxide: an endogenous modulator of sinusoidal tone in the perfused rat liver. J Clin Invest 1995;96:2431-2437.
3. Ozawa N, Goda N, Makino N, Yamaguchi T, Yoshimura Y, Suematsu M. Leydig cell-derived heme oxygenase-1 regulates apoptosis of premeiotic germ cells in response to stress. J Clin Invest 2002;109:457-467.
4. Song R, Zhou Z, Kim PK, Shapiro RA, Liu F, Ferran C, et al. Carbon monoxide promotes Fas/CD95-induced apoptosis in Jurkat cells. J Biol Chem 2004;279:44327-44334.
5. Mori M, Suematsu M, Kyokane T, Sano T, Suzuki H, Yamaguchi T, et al. Carbon monoxide-mediated alterations in paracellular permeability and vesicular transport in acetaminophen-treated perfused rat liver. HEPATOLOGY 1999;30:160-168.
6. Kyokane T, Norimizu S, Taniai H, Yamaguchi T, Takeoka S, Tsuchida E, et al. Carbon monoxide from heme catabolism protects against hepatobiliary dysfunction in endotoxin-treated rat liver. Gastroenterology 2001;120:1227-1240.
7. Zhao Y, Brandish PE, Ballou DP, Marletta MA. A molecular basis for nitric oxide sensing by soluble guanylate cyclase. Proc Natl Acad Sci U S A 1999;96:14753-14758.
8. Otterbein LE, Bach FH, Alam J, Soares M, Tao Lu H, Wysk M, et al. Carbon monoxide has anti-inflammatory effects involving the mitogen-activated protein kinase pathway. Nat Med 2000;6:422-428.
9. Abraham NG, Quan S, Mieyal PA, Yang L, Burke-Wolin T, Mingone CJ, et al. Modulation of cGMP by human HO-1 retrovirus gene transfer in pulmonary microvessel endothelial cells. Am J Physiol Lung Cell Mol Physiol 2002;283:L1117-L1124.
10. Hill M, Pereira V, Chauveau C, Zagani R, Remy S, Tesson L, et al. Heme oxygenase-1 inhibits rat and human breast cancer cell proliferation: mutual cross inhibition with indoleamine 2,3-dioxygenase. FASEB J 2005;19:1957-1968.
11. Thomas SR, Mohr D, Stocker R. Nitric oxide inhibits indoleamine 2,3-dioxygenase activity in interferon-gamma primed mononuclear phagocytes. J Biol Chem 1994;269:14457-14464.
12. Shinoda Y, Suematsu M, Wakabayashi Y, Suzuki T, Goda N, Saito S, et al. Carbon monoxide as a regulator of bile canalicular contractility in cultured rat hepatocytes. HEPATOLOGY 1998;28:286-295.
13. Wakabayashi Y, Takamiya R, Mizuki A, Kyokane T, Goda N, Yamaguchi T, et al. Carbon monoxide overproduced by heme oxygenase-1 causes a reduction of vascular resistance in perfused rat liver. Am J Physiol 1999;277:G1088-G1096.
14. Fujii K, Sakuragawa T, Kashiba M, Sugiura Y, Kondo M, Maruyama K, et al. Hydrogen sulfide as an endogenous modulator of biliary bicarbonate excretion in the rat liver. Antioxid Redox Signal 2005;7:788-794.
15. Vreman HJ, Wong RJ, Kadotani T, Stevenson DK. Determination of carbon monoxide (CO) in rodent tissue: effect of heme administration and environmental CO exposure. Anal Biochem 2005;341:280-289.

16. Motterlini R, Clark JE, Foresti R, Sarathchandra P, Mann BE, Green CJ. Carbon monoxide-releasing molecules: characterization of biochemical and vascular activities. Circ Res 2002;90:e17-e24.
17. Bossard R, Stieger B, O'Neill B, Fricker G, Meier PJ. Ethinylestradiol treatment induces multiple canalicular membrane transport alterations in rat liver. J Clin Invest 1993;91:2714-2720.
18. Soga T, Baran R, Suematsu M, Ueno Y, Ikeda S, Sakurakawa T, et al. Differential metabolomics reveals ophthalmic acid as an oxidative stress biomarker indicating hepatic glutathione consumption. J Biol Chem 2006;281:16768-16776.
19. Kinoshita A, Tsukada K, Soga T, Hishiki T, Ueno Y, Nakayama Y, et al. Roles of hemoglobin allostery in hypoxia-induced metabolic alterations in erythrocytes: simulation and its verification by metabolome analysis. J Biol Chem 2007;282:10731-10741.
20. Goda N, Suzuki K, Naito M, Takeoka S, Tsuchida E, Ishimura Y, et al. Distribution of heme oxygenase isoforms in rat liver: topographic basis for carbon monoxide-mediated microvascular relaxation. J Clin Invest 1998; 101:604-612.
21. Yonetani T, Tsuneshige A, Zhou Y, Chen X. Electron paramagnetic resonance and oxygen binding studies of alpha-nitrosyl hemoglobin: a novel oxygen carrier having NO-assisted allosteric functions. J Biol Chem 1998; 273:20323-20333.
22. Suganuma K, Tsukada K, Kashiba M, Tsuneshige A, Furukawa T, Kubota T, et al. Erythrocytes with T-state-stabilized hemoglobin as a therapeutic tool for postischemic liver dysfunction. Antioxid Redox Signal 2006;8: 1847-1855.
23. Meier M, Janosik M, Kery V, Kraus JP, Burkhard P. Structure of human cystathionine beta-synthase: a unique pyridoxal 5'-phosphate-dependent heme protein. EMBO J 2001;20:3910-3916.
24. Taoka S, Banerjee R. Characterization of NO binding to human cystathionine beta-synthase: possible implications of the effects of CO and NO binding to the human enzyme. J Inorg Biochem 2001;87:245-251.
25. Prudova A, Bauman Z, Braun A, Vitvitsky V, Lu SC, Banerjee R. S-adenosylmethionine stabilizes cystathionine beta-synthase and modulates redox capacity. Proc Natl Acad Sci USA 2006;103:6489-6494.
26. Zhao W, Zhang J, Lu Y, Wang R. The vasorelaxant effect of H_2S as a novel endogenous gaseous K_{ATP} channel opener. EMBO J 2001;20:6008-6016.
27. Werstuck GH, Lentz SR, Dayal S, Hossain GS, Sood SK, Shi YY, et al. Homocysteine-induced endoplasmic reticulum stress causes dysregulation of the cholesterol and triglyceride biosynthetic pathways. J Clin Invest 2001;107:1263-1273.
28. Maher JM, Dieter MZ, Aleksunes LM, Slitt AL, Guo G, Tanaka Y, et al. Oxidative and electrophilic stress induces multidrug resistance-associated protein transporters via the nuclear factor-E2-related factor-2 transcriptional pathway. HEPATOLOGY 2007;46:1597-1610.
29. Sasaki H, Sato H, Kuriyama-Matsumura K, Sato K, Maebara K, Wang H, et al. Electrophile response element-mediated induction of the cystine/glutamate exchange transporter gene expression. J Biol Chem 2002;277: 44765-44771.
30. Fiorucci S, Antonelli E, Mencarelli A, Orlandi S, Renga B, Rizzo G, et al. The third gas: H_2S regulates perfusion pressure in both the isolated and perfused normal rat liver and in cirrhosis. HEPATOLOGY 2005;42:539-548.
31. Suematsu M, Ishimura Y. The heme oxygenase-carbon monoxide system: a regulator of hepatobiliary function. HEPATOLOGY 2000;31:3-6.
32. Kato Y, Shimazu M, Kondo M, Uchida K, Kumamoto Y, Wakabayashi G, et al. Bilirubin rinse: a simple protectant against the rat liver graft injury mimicking heme oxygenase-1 preconditioning. HEPATOLOGY 2003;38:364-373.
33. Sano T, Shiomi M, Wakabayashi Y, Shinoda Y, Goda N, Yamaguchi T, et al. Endogenous carbon monoxide suppression stimulates bile acid-dependent biliary transport in perfused rat liver. Am J Physiol 1997;272:G1268-G1275.
34. Norimizu S, Kudo A, Kajimura M, Ishikawa K, Taniai H, Yamaguchi T, et al. Carbon monoxide stimulates mrp2-dependent excretion of bilirubin-IXα into bile in the perfused rat liver. Antioxid Redox Signal 2003;5:449-456.
35. Nathanson MH, Burgstahler AD, Mennone A, Dranoff JA, Rios-Velez L. Stimulation of bile duct epithelial secretion by glybenclamide in normal and cholestatic rat liver. J Clin Invest 1998;101:2665-2676.
36. Spirli C, Fiorotto R, Song L, Santos-Sacchi J, Okolicsanyi L, Masier S, et al. Glibenclamide stimulates fluid secretion in rodent cholangiocytes through a cystic fibrosis transmembrane conductance regulator-independent mechanism. Gastroenterology 2005;129:220-233.
37. Sellers ZM, Mann E, Smith A, Ko KH, Giannella R, Cohen MB, et al. Heat-stable enterotoxin of Escherichia coli (STa) can stimulate duodenal HCO_3^- secretion via a novel GC-C- and CFTR-independent pathway. FASEB J 2008;22:1306-1316.
38. Boon EM, Huang SH, Marletta MA. A molecular basis for NO selectivity in soluble guanylate cyclase. Nat Chem Biol 2005;1:53-59.
39. Kajimura M, Shimoyama M, Tsuyama S, Suzuki T, Kozaki S, Takenaka S, et al. Visualization of gaseous monoxide reception by soluble guanylate cyclase in the rat retina. FASEB J 2003;17:506-508.
40. Imai T, Morita T, Shindo T, Nagai R, Yazaki Y, Kurihara H, et al. Vascular smooth muscle cell-directed overexpression of heme oxygenase-1 elevates blood pressure through attenuation of nitric oxide-induced vasodilation in mice. Circ Res 2001;89:55-62.
41. Ishikawa M, Kajimura M, Adachi T, Maruyama K, Makino N, Goda N, et al. Carbon monoxide from heme oxygenase-2 is a tonic regulator against NO-dependent vasodilatation in the adult rat cerebral microcirculation. Circ Res 2005;97:e104-e114.

Inhibiting nitric oxide overproduction during hypotensive sepsis increases local oxygen consumption in rat skeletal muscle*

Ryon M. Bateman, PhD; Michael D. Sharpe, MD; Daniel Goldman, PhD; Darcy Lidington, PhD; Christopher G. Ellis, PhD

Objective: **Although nitric oxide (NO) is a known regulator of cardiovascular function, the effect of NO overproduction during sepsis on capillary oxygen transport and local tissue oxygen consumption is not well understood. The objectives of this study were to determine whether sepsis-induced NO overproduction increased capillary stopped-flow and modulated tissue oxygen consumption in skeletal muscle.**

Design: **Prospective, controlled laboratory study.**

Setting: **Animal laboratory in a university-affiliated research institute.**

Subjects: **Male Sprague-Dawley rats, 165–180 g body weight.**

Interventions: **Rats were made septic by cecal ligation and perforation (CLP) and were then ventilated and volume resuscitated (saline). The hind limb extensor digitorum longus (EDL) skeletal muscle was blunt dissected for *in vivo* microvascular imaging. The inducible NO synthase (iNOS) inhibitor L-N6-(1-iminoethyl)lysine dihydrochloride (L-NIL) was infused (3 mg/kg body weight per hour) starting 1 hr post-CLP to maintain arterial blood and EDL tissue NO_x^- (NO_2^- + NO_3^-) at baseline.**

Measurements and Main Results: **Red blood cell hemodynamics, hemoglobin oxygen saturation, capillary geometry, and functional capillary density information were used to calculate capillary oxygen flux (the rate of oxygen diffusion from capillary to tissue) and indices of local oxygen delivery and tissue oxygen consumption. Over the first 5 hrs of septic injury, mean arterial pressure decreased while capillary stopped-flow and capillary oxygen flux both increased ($p < .05$). Inhibiting iNOS/NO overproduction partially restored mean arterial pressure and increased arterial pH. Within the microcirculation, inhibiting NO increased capillary red cell velocity and increased local tissue oxygen consumption ($p < .05$). Inhibiting NO failed, however, to prevent capillary stopped-flow.**

Conclusions: **During the onset of sepsis, concurrent with the onset of microvascular dysfunction, there is an iNOS/NO-mediated reduction in local skeletal muscle tissue oxygen consumption. (Crit Care Med 2008; 36:225–231)**

KEY WORDS: **sepsis; microcirculation; nitric oxide; capillaries; oxygen consumption**

Nitric oxide (NO) is a gas produced from L-arginine and oxygen. During sepsis, the overproduction of NO due to upregulation of inducible NO synthase (iNOS) has been associated with impaired vascular reactivity, capillary leak, decreased erythrocyte deformability, and refractory hypotension (1). *In vitro* experiments have shown that NO inhibits mitochondrial respiration both reversibly and irreversibly, depending on the duration of NO exposure and the mitochondrial complex inhibited (2–5), thereby reducing oxygen consumption. The reversible NO-mediated inhibition of cytochrome *c* oxidase (complex IV) depends on oxygen concentration (5), which *in vivo* would be established by local capillary oxygen delivery and tissue oxygen consumption. Whether iNOS/NO overproduction modulates local *in vivo* tissue oxygen consumption during sepsis is unknown.

Nonspecific NOS inhibition was found to reduce tissue P_{O_2} in skeletal muscle in septic rats (6) and the hind limb of normal dogs (7), whereas more specific iNOS inhibition was found to increase serosal microvascular oxygenation in endotoxemic pigs (8). Initial clinical studies reported that nonspecific NOS inhibition normalized cardiac output and systemic vascular resistance while reducing vasopressor use, without any apparent adverse effects on tissue oxygenation or organ function (9, 10). Seemingly in agreement were the open-label dose escalation study and clinical trial of the nonspecific NOS inhibitor 546C88, which found that while global oxygen extraction increased, oxygen consumption was maintained (11–13). In contrast, Statman et al. (14) reported that nonspecific NOS inhibition increased systemic vascular resistance at the expense of tissue oxygenation in septic patients. While the ultimate failure of the multicenter clinical trial of 546C88 was attributed to cardiovascular death (12), what is not understood in sepsis, in either patients or experimental models, is the overall effect of iNOS/NO overproduction and its inhibition on microvascular oxygen transport and local ox-

*See also p. 359.

From the University of Western Ontario and the London Health Sciences Centre, Department of Medical Biophysics (RMB, DL, CGE) and Department of Anesthesia and Program in Critical Care Medicine (MDS), London, ON, Canada; and the Departments of Mathematical Sciences and Biomedical Engineering, New Jersey Institute of Technology, Newark, NJ (DG).

Supported, in part, by research grant MOP-499416 from the Canadian Institutes of Health, London, ON, Canada. University of Western Ontario (CGE). Dr. Bateman is a Lewis MacDonald Research Fellow and was supported by the Spoerel Research Fellowship (London, ON, Canada) and the Heart and Stroke Foundation of Canada (postdoctoral fellowship). The authors have not disclosed any potential conflicts of interest.

Address requests for reprints to: Ryon M. Bateman, PhD, Department of Biochemistry and Integrative Medical Biology, School of Medicine, Keio University, 35 Shinanomachi, Shinjuku-Ku, Tokyo 160-8582 Japan.

DOI: 10.1097/01.CCM.0000295307.92027.2F